

Coupling of Aromatic Aldehydes with CO₂Me-Substituted Tp^{Me₂}Ir(III) Metallacyclopentadienes

Arián E. Roa,^{†,‡} Verónica Salazar,^{‡,*} Joaquín López-Serrano,[†] Enrique Oñate,[‡] José G. Alvarado-Rodríguez,[‡] Margarita Paneque,^{†,*} and Manuel L. Poveda[†]

[†] Instituto de Investigaciones Químicas (IIQ) and Departamento de Química Inorgánica, CSIC and Universidad de Sevilla, Av. Américo Vespucio 49, 41092 Sevilla, Spain

[‡] Centro de Investigaciones Químicas, Universidad Autónoma del Estado de Hidalgo, Carretera Pachuca a Tulancingo Km 4.5, 42184 Mineral de la Reforma, Hidalgo, México

[‡] Departamento de Química Inorgánica and Instituto de Síntesis Química y Catálisis Homogénea (ISQCH), Universidad de Zaragoza and CSIC, 50009 Zaragoza, Spain

RECEIVED DATE

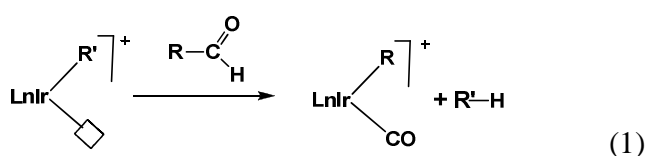
ABSTRACT: The fully CO₂Me-substituted aquo-iridacyclopentadiene **1** reacts with a variety of aromatic aldehydes, at 90-120 °C, with formation of bicyclic Fischer-type carbenes, generated by the transfer of the aldehydic H atom to a α -carbon of the metallacycle and concomitant bonding of the O-atom to the adjacent β -carbon. These carbenes have a thermodynamically favored *anti* configuration of these C—H and C—O bonds but it is proposed that an unobserved *syn* carbene is the kinetic primary product, which then easily epimerizes by adventitious water. Milder reaction conditions, 25-60 °C, allow for the isolation of intermediate *O*-coordinated aldehyde adducts. While these reactions have been observed for a wide variety of aromatic aldehydes, 2-pyridinecarboxaldehyde behaves differently as the

reaction leads to a very stable *N*-adduct, in spite of two isomeric *O*-bonded adducts being formed as kinetic products,.

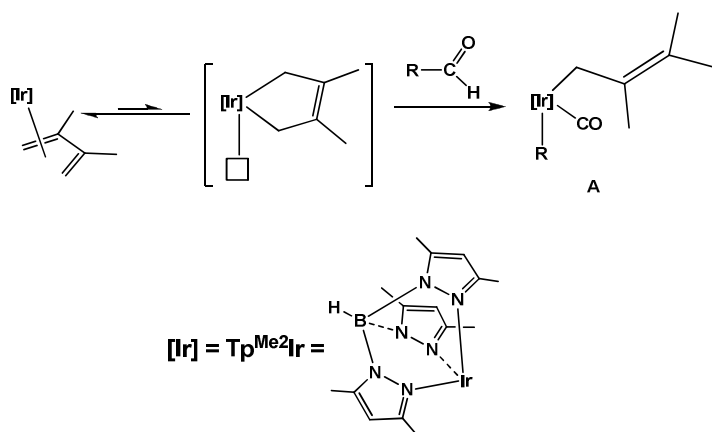
INTRODUCTION

Aldehydes are very important substrates in synthetic organic chemistry, as they can experience different types of transformations. The simple, normally metal-mediated, aldehyde decarbonylation^{1,2} ($\text{R}-\text{C}(\text{O})\text{H} \rightarrow \text{R}-\text{H} + \text{CO}$) is receiving increasing interest as more additional examples of the coupling of this process with different reactions are being developed.³ Many more examples besides this report the use of aldehydes in other processes such as their dimerization to esters (Tishchenko reaction),⁴ the preparation of biofuels from carbohydrate feedstock,⁵ asymmetric synthesis,⁶ the application as CO releasing molecules (CORM's),⁷ etc.

Rh(I) and Ir(I) complexes are well known for their ability to effect, either stoichiometric or catalytically, the decarbonylation of aldehydes.⁸ If Ir(III)-R species are considered it has been found that, provided that there is a vacant coordination position easily available, their reaction with aldehydes afford carbonyl-Ir(III) complexes. This is best exemplified by the work of Bergman *et al.* in a cationic $(\text{C}_5\text{Me}_5)\text{Ir}$ system⁹ which is summarized in eq 1.

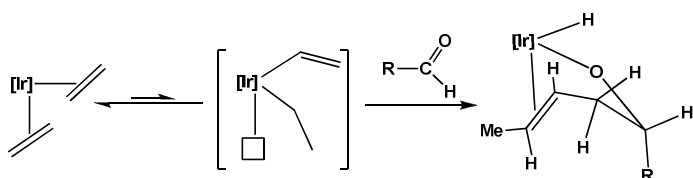


In the $\text{Tp}^{\text{Me}_2}\text{Ir}(\text{III})$ system, we have reported on a similar behavior on the reaction of the diene derivative $\text{Tp}^{\text{Me}_2}\text{Ir}(\text{CH}_2=\text{C}(\text{Me})\text{C}(\text{Me})=\text{CH}_2)$ with aliphatic and aromatic aldehydes, eventually yielding the Ir(III) carbonyl species **A** shown in Scheme 1, in a reaction that takes place first by formation of the 16 e^- unsaturated Ir(III) species shown in the Scheme and then through a series of kinetic bicyclic Fischer carbene "intermediates" to be commented in more detail below.¹⁰



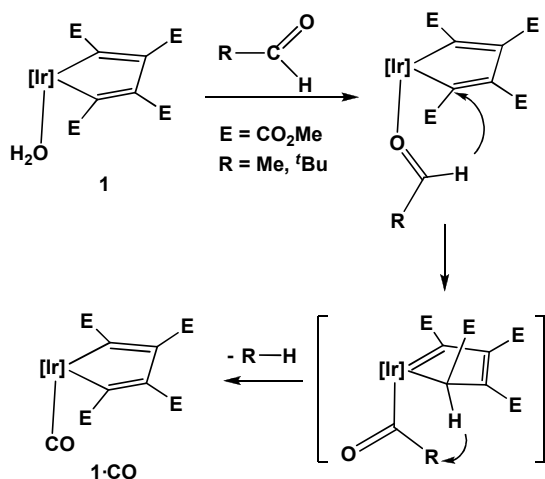
Scheme 1. Reactivity of $\text{Tp}^{\text{Me}_2}\text{Ir}(\text{CH}_2=\text{C}(\text{Me})\text{C}(\text{Me})=\text{CH}_2)$ with aldehydes (refer. 10). Throughout the paper, $[\text{Ir}]$ represents $\text{Tp}^{\text{Me}_2}\text{Ir}$ (Tp^{Me_2} = hydrotris(3,5-dimethylpyrazolyl)borate).

However, a different outcome was observed on the reaction of the complex $\text{Tp}^{\text{Me}_2}\text{Ir}(\text{C}_2\text{H}_4)_2$ with the same substrates, in which, through the participation of the 16 e^- unsaturated Ir(III) species shown in Scheme 2, an interesting coupling took place. In this case, the aldehyde experienced a nucleophilic attack of an alkenyl ligand, with the eventual formation of an elaborated chelating ligand.¹¹



Scheme 2. Reactivity of $\text{Tp}^{\text{Me}_2}\text{Ir}(\text{C}_2\text{H}_4)_2$ with aldehydes (refer. 11).

Very recently, we have described the thermal reactions of the fully CO_2Me substituted Ir(III) metallacyclopentadiene **1** with aliphatic aldehydes $\text{RC}(\text{O})\text{H}$ ($\text{R} = \text{Me}, \text{tBu}$), which result on the decarbonylation of the organic substrate as depicted in Scheme 3. These findings were rationalized on the basis of a reversible abstraction-donation of the aldehydic hydrogen of the corresponding *O*-adduct by a α -carbon of the iridacycle (Scheme 3).¹²



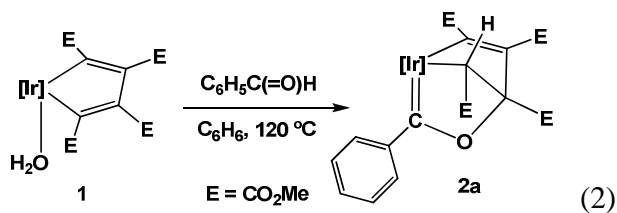
Scheme 3. Reaction of **1** with aliphatic aldehydes (refer. 12).

In this contribution, we report on the very different reactivity that complex **1** shows against aromatic aldehydes, which lead to an interesting set of Ir(III) Fischer carbenes that resemble those obtained as intermediates in the reaction of Scheme 1 (see below).

RESULTS AND DISCUSSION

Formation of bicyclic Fischer carbenes

The reaction of the iridacycle **1**¹³ with benzaldehyde (1.5 equiv., C₆H₆, 120 °C) leads to the bicyclic compound **2a** in almost quantitative spectroscopic (NMR) yield (eq 2).



As can be observed, **2a** is the result of an interesting coupling of the iridacyclopentadiene, after extrusion of water, with the aldehyde. The latter functionality has been transformed into a Fischer carbene ligand with its oxygen being bonded to one of the β -carbons of the original metallacycle and with the aldehydic hydrogen being stereoselectively transferred to the adjacent α carbon, *anti* with respect to the formed O—C bond. Species **2a** has been completely characterized by spectroscopy

methods including single crystal X-ray diffraction studies. Inspection of both the ^1H and ^{13}C NMR spectra immediately reveals the lack of the 2:1 symmetry exhibited by the starting material **1** and thus independent resonances are observed for the nuclei of each of the pyrazolyl arms of the Tp^{Me_2} ligand. In the ^1H NMR spectrum, the most characteristic resonance is a singlet at 5.24 ppm that corresponds to the Ir-CH(E)- proton that derives from the aldehydic H atom. In the $^{13}\text{C}\{^1\text{H}\}$ NMR the supporting sp^3 carbon of this proton resonates at 33.6 ppm ($^1J_{\text{CH}} = 138$ Hz) while the carbene carbon gives rise to a signal at 252.3 ppm.

Figure 1 shows an ORTEP representation of the molecular structure of **2a**, together with some selected bond distances and angles. The carbene ligand has a bond distance Ir—C(16) of 1.929(5) Å while the other two Ir—C bonds have lengths of 2.107(5) Å (Ir—CH(E)-C(E)-) and 2.031(5) Å (Ir—C(E)=C(E)-) respectively, which fall within the expected range for these types of single bonds.¹⁴

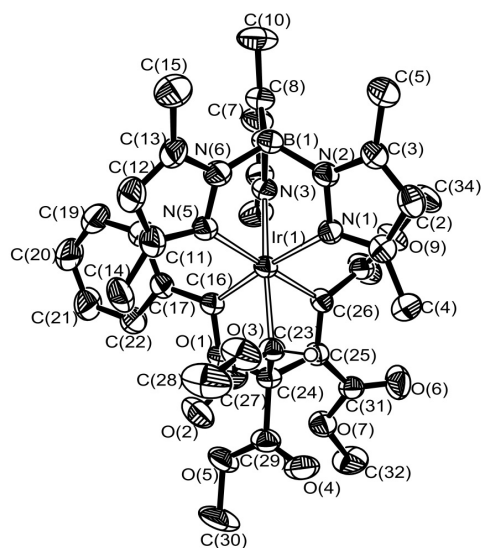
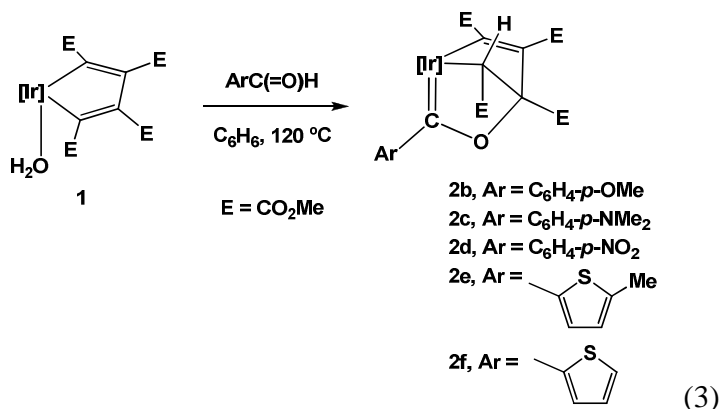


FIGURE 1. X-ray structure of compound **2a** (50% displacement ellipsoids, H atoms except the H atom on C(23) omitted for clarity). Selected bond lengths (Å) and angles (deg): Ir(1)—C(16) 1.929(5), Ir(1)—C(26) 2.031(5), Ir(1)—C(23) 2.107(5), Ir(1)—N(1) 2.160(4), Ir(1)—N(3) 2.160(4), Ir(1)—N(5) 2.167(4), C(25)—C(26) 1.342(7); C(16)—Ir(1)-C(26) 86.3(2), C(16)—Ir(1)—C(23) 79.0(2), C(26)—Ir(1)—C(23) 77.7(2).

Similar reaction outcomes as the one depicted in eq 2 take place with a variety of aromatic aldehydes. Thus, anisaldehyde, *p*-dimethylaminobenzaldehyde, *p*-nitrobenzaldehyde, and two thienylaldehydes provide the related compounds **2b-f** in excellent spectroscopic yields (eq 3).



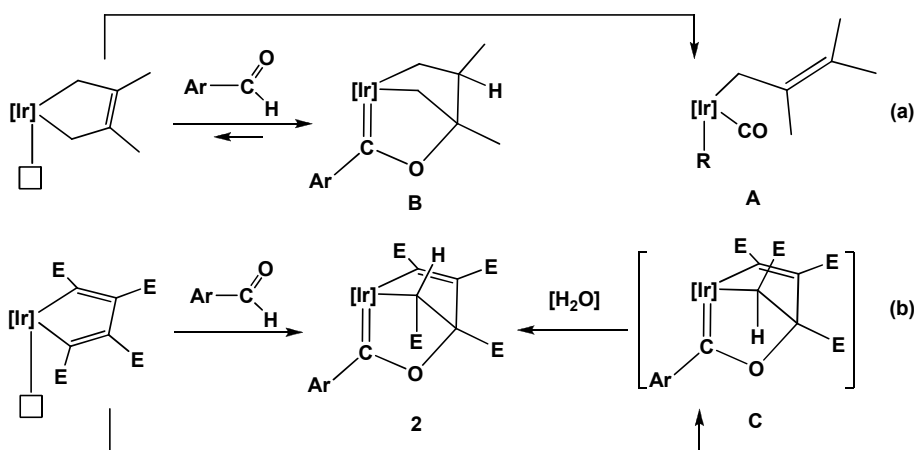
Probably due to steric reasons, the rotation around the C–Ar bond of the aromatic residue on the carbene ligand is slow, at 25 °C, on the NMR time scale. For the case of the thienyl-derived compounds only one of the two possible rotamers is present in CDCl₃ solution, and this is the one with the sulfur pointing away from the Tp^{Me2} ligand.

Interestingly in all the carbenes studied, of the four non-equivalent CO₂Me groups, the methyl resonances appearing at lower field in both the ¹H and ¹³C{¹H} NMR spectra are broadened. This broadening also affects to the corresponding CO₂Me nuclei and for that reason they remain unobserved in the ¹³C{¹H} NMR spectra but can be detected by a weak cross peak in the ¹H-¹³C HMBC spectrum. This behavior is best explained by invoking that the particular CO₂Me group populates two, or more, conformers that, at ambient temperature, are not in the rapid exchange regime on the NMR time scale, but no efforts have been devoted to either clarify this issue or to positively identify the responsible CO₂Me group.

Electron withdrawing substituents in the aldehyde favors the coupling reaction of eq 3 and thus we have found that **1** and *p*-NO₂-C₆H₄C(=O)H react in C₆D₆ solution at 90 °C, under pseudo-first order conditions (25 mM, 5 equiv. aldehyde), to give **2d** with *t*_{1/2} of *ca.* 30 min, while *p*-OMe-C₆H₄C(=O)H does so, at 120 °C, with *t*_{1/2} of *ca.* 1 h. As expected, and following this trend, the more powerful electron-donating NMe₂ substituent retards the coupling even more (120 °C, *t*_{1/2} of *ca.* 18 h). Heating

compounds **2** at a temperature higher than needed for their formation (150 °C) only results in a slow decomposition to a complex mixture of unidentified products, at least for the compounds tested, **2a** and **2d**.

In comparing the reactivity, against aromatic aldehydes, of complex **1** and also of the Tp^{Me2}-iridacyclopentene commented on in the Introduction, two questions arise. First, in route to the carbonyl derivatives Tp^{Me2}Ir(Ar)(CH₂C(Me)=CMe₂)(CO) (**A**), bicyclic compounds **B** related to **2** were isolated as "intermediate species" (Scheme 4) where the aldehydic hydrogen was added in a *syn* disposition with respect to the formed O—C bond and this may be called a "normal" transfer of this hydrogen; so, why this stereochemistry is not observed in species **2**?

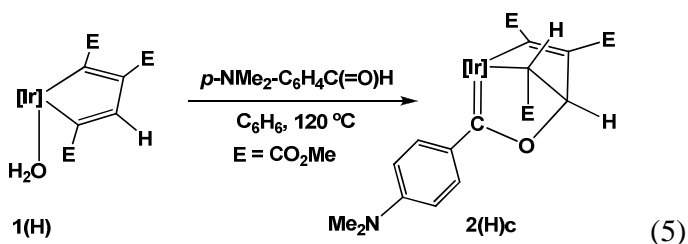
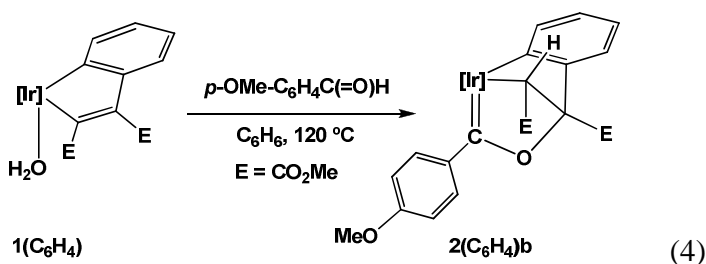


Scheme 4. Comparison of the bicyclic carbene structures obtained in reference 10 (a) and in this work (b).

DFT calculations are clearly in accord with the fact that the *anti* stereoisomer **2** is more stable than the unobserved *syn* addition product **C** (by 6.9 kcal·mol⁻¹) and we propose that this species is the primary reaction product, although one that experiences an easy **C**→**2** epimerization by adventitious water acting as a basic transfer catalyst. Evidence for this mechanism was found by heating complex **2a** in C₆D₆ containing CD₃OD, where complete deuteration of the CH(CO₂Me) functionality was observed after 1 h at 120 °C.

The second question concerns the lack of a clean decarbonylation of carbenes **2**, under forced conditions. In comparison, this process was observed for derivatives **B**,¹⁰ and more remarkably it was also the case when the same precursor **1** reacted, at 120 °C, with aliphatic aldehydes (acetaldehyde and ^tBu-aldehyde) where the Ir-carbonyl **1**•CO and the corresponding alkane were formed¹² (see Schemes 1 and 3 in the Introduction). We have tried to understand this dichotomy through the use of DFT calculations to be described below.

Related metallacycles also experience this type of coupling. Thus, the benzo-annulated iridacyclopentadiene **1**(C₆H₄)¹⁵ provides the corresponding carbene upon reacting with *p*-anisaldehyde (eq 4), while the three-CO₂Me-substituted derivative **1**(H)¹⁶ does the same upon reacting with *p*-NMe₂-C₆H₄C(=O)H (eq 5). Once again, in both complexes the aldehydic hydrogen appears in an *anti* relationship with respect to the formed O—C moiety.



As can be observed, formation of complex **2**(H)**c** implies the selective binding of the aldehydic oxygen atom to the β -carbon that bears the hydrogen atom. This regioselectivity is accompanied by an increase of the reactivity of complex **1**(H) with respect to **1** as **2**(H)**c** is formed *ca.* one order of magnitude faster than the corresponding **2c**. This may be the result of the H transfer being subjected to

less steric pressure, but also because the attacked Ir-C(E)=C(H)- moiety is less electronically poor. This latter factor complements the reactivity results obtained upon changing the nature of the aldehyde (see above)

Compounds **2(C₆H₄)b** and **2(H)c** have been completely characterized from spectroscopic data and, in the case of **2(C₆H₄)b**, by a single-crystal X-ray structure determination (Figure 3). In this complex the Ir(1)—C(1), Ir(1)—C(16) and Ir(1)—C(10) bond lengths (1.918(6), 2.021(6) and 2.137(6) Å respectively) are in the range expected for Ir-carbene, Ir-alkenyl and Ir-alkyl functionalities.¹⁷ The C—Ir—C bite angles are 87.3(2)° (C(1)—Ir(1)—C(16)), 78.7(2)° (C(1)—Ir(1)—C(10)) and 77.5(2)° (C(10)—Ir(1)—C(16)) for the different metallacycles.

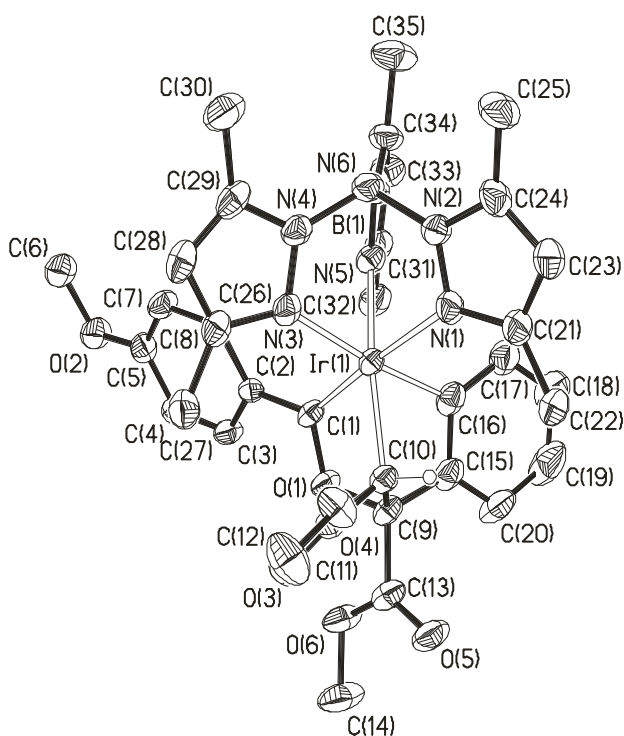
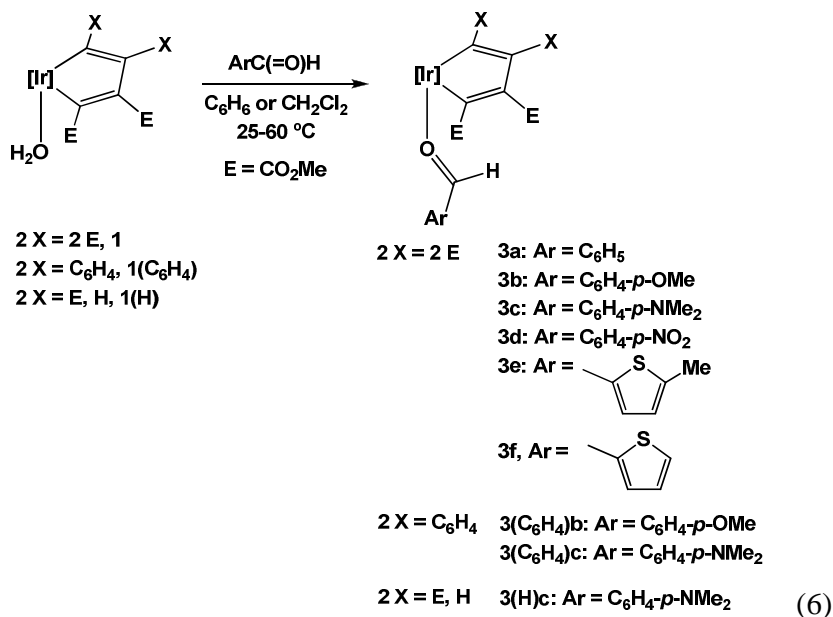


Figure 3. X-ray structure of compound **2(C₆H₄)b** (50% displacement ellipsoids, H atoms except the H atom on C(10) omitted for clarity). Selected bond lengths (Å) and angles (deg): Ir(1)—C(1) 1.918(6), Ir(1)—C(16) 2.021(6), Ir(1)—C(10) 2.137(6), C(16)—C(15) 1.392(9), C(15)—C(9) 1.501(9); C(1)—Ir(1)—C(16) 87.3(2), C(1)—Ir(1)—C(10) 78.7(2), C(10)—Ir(1)—C(16) 77.5(2).

Isolation of intermediate *O*-coordinated aldehyde adducts

If the reactions of eqs 2-5 are conducted under milder conditions in C₆H₆ or CH₂Cl₂ (25-60 °C), the *O*-coordinated aldehyde adducts **3** are formed instead (eq 6). These species are easily characterized by NMR. All of them exhibit a ¹H NMR resonance around 9-10 ppm (see Experimental) corresponding to the aldehydic H atom, *i.e.* at values close to those of the free aldehydes, and the same is true for the resonances corresponding to the aldehydic C nuclei. These data indicate η¹-*O*-coordination of the aldehydes¹⁸ and we observe, as expected, that in the presence of the thienyl moieties, Ir(III) prefers to coordinate with the aldehydic oxygen rather than with the softer sulfur atom. In all these compounds, the aryl ring of the aldehyde rotates fast, around the Ar—C bond at 25 °C, on the NMR time scale, and NOESY spectra (see graphics in the Experimental Section) indicate that the aldehydic hydrogen is pointing towards the metallacycle as is depicted in eq 6.



The reactivity of complex **1** against selected aldehydes has been studied by monitoring the formation of the *O*-adducts, in CD₂Cl₂ at 25 °C, under pseudo first-order conditions (25 mM, *ca* 5 equiv. of aldehyde). Rather surprisingly, and as was the case for the formation of complexes **2**, electron withdrawing substituents in the aryl ring of the benzaldehyde kinetically favor *O*-adduct formation and thus the following reactivity order has been found: *p*-NO₂-C₆H₄C(=O)H > C₆H₅C(=O)H > *p*-OMe-C₆H₄C(=O)H (after 24 h, the corresponding adducts were formed in 90, 50 and 20%, respectively).

However this sequence is reverted, as expected, when the reactions are under thermodynamic control and thus it has been found for example that at 60 °C, in CDCl₃, the equilibrium **3d** + *p*-OMe-C₆H₄C(=O)H \rightleftharpoons **3b** + *p*-NO₂-C₆H₄C(=O)H (25 mM, 5 equiv. of each aldehyde) is set up after *ca.* 10 h with *K* = 13.

The *O*-coordinated aldehyde structure has been confirmed in the solid state by an X-ray study carried out with compound **3b**. Figure 4 shows an ORTEP view of this derivative, along with some selected bond distances and angles. The metallacycle moiety is not affected by the coordination of the aldehyde, and the bond distances and angles are almost identical to those found in the parent compound **1**.¹⁴ The X-ray study also indicates that the rotamer present in solution, *i.e.* the one with the aldehydic C—H pointing towards the metallacycle, is also the one favoured in solid state. As can be observed, this disposition situates the aryl ring far away from the crowded metal-ligand environment, thus accounting for its free rotation observed by NMR. Other bond distances and angles fall within the expected values and need no further comment.

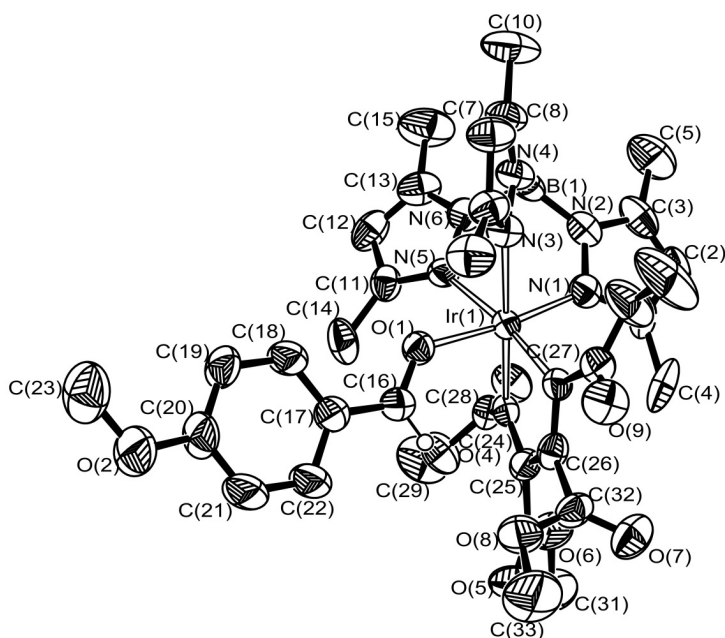


Figure 4. X-ray structure of compound **3b** (50% displacement ellipsoids, H atoms except the H atom on C(16) omitted for clarity). Selected bond lengths (Å) and angles (deg): Ir(1)—C(24) 2.029(8),

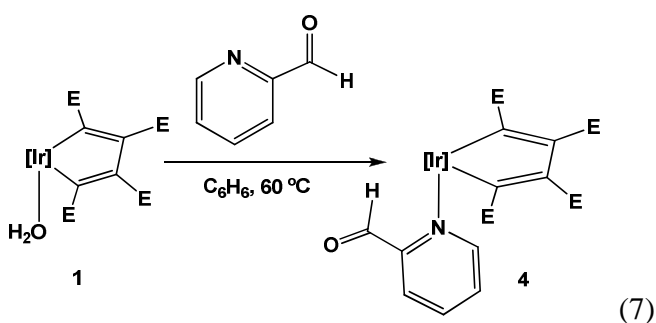
Ir(1)—C(27) 2.032(8), Ir(1)—N(1) 2.037(8), Ir(1)—O(1) 2.074(6), Ir(1)—N(5) 2.144(7), Ir(1)—N(3) 2.150(7); C(24)—Ir(1)—C(27) 79.5(3).

The *O*-bonded aldehyde ligands are labile, as shown in the above-mentioned equilibration studies, and in some cases they may revert to the corresponding aldehyde and compound **1**. This may prevent the proper purification and spectral characterization of some compounds **3**, unless a significant amount of the corresponding free aldehyde is present in their solutions.

Upon heating in solution (C_6H_6 , 90-120 °C), the adducts of eq 6 transform into the corresponding carbenes **2**. No intermediate species could be identified through monitoring the reactions by NMR, only the adducts **3** and the final carbenes **2** being observed throughout the process. Thus, the mechanism of the coupling reactions was investigated by DFT (see below).

The case of 2-pyridinecarboxaldehyde

The reaction of **1** with 2-pyridinecarboxaldehyde provides quite different results to those described so far. At 60 °C, it results in the formation of the *N*-adduct **4** (eq 7).



Compound **4** is characterized in the 1H NMR spectrum by the chemical shift of the aldehydic H atom at 6.88 ppm. This value is clearly shifted to a higher field with respect to the *O*-adducts described above, thus indicating that this functionality in **4** is in a different chemical environment. The NOESY experiment reveals an interaction between this H atom and two of the pyrazolyl methyl groups, thereby supporting that **4** is adopting the rotameric structure shown in eq 7. Furthermore, we have already

noticed that protons placed between two pyrazolyl arms of the Tp^{Me_2} ligand experience considerable shielding due to the electronic ring currents of the heterocycles.

The bonding of the 2-pyridinecarboxaldehyde ligand in **4** was ascertained by single crystal X-ray diffraction studies. In Figure 5, the molecular structure of this complex is represented, and the selected bond distances and angles collected are very similar to those observed in previously reported $\text{Tp}^{\text{Me}_2}\text{Ir(III)}$ adducts¹⁹ of 2-substituted pyridines. The iridacyclopentadiene unit is almost planar, with a bite angle of $78.92(12)^\circ$, and the Ir—C bond lengths are 2.021(3) and 2.030(3) Å, as expected for Ir(III)-bound sp^2 carbon atoms. Due to the lower *trans* influence of the pyridine, the Ir—N(pyrazolyl) bond *trans* to it is shorter (2.066(2) Å) than the other two (2.132(2) and 2.162(3) Å).

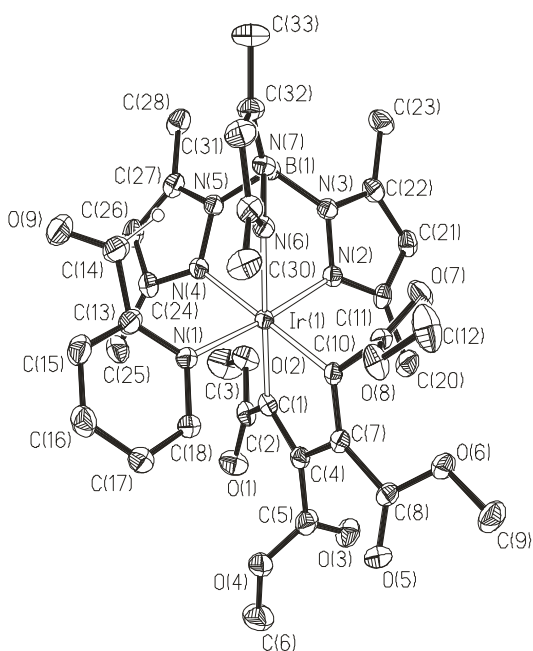
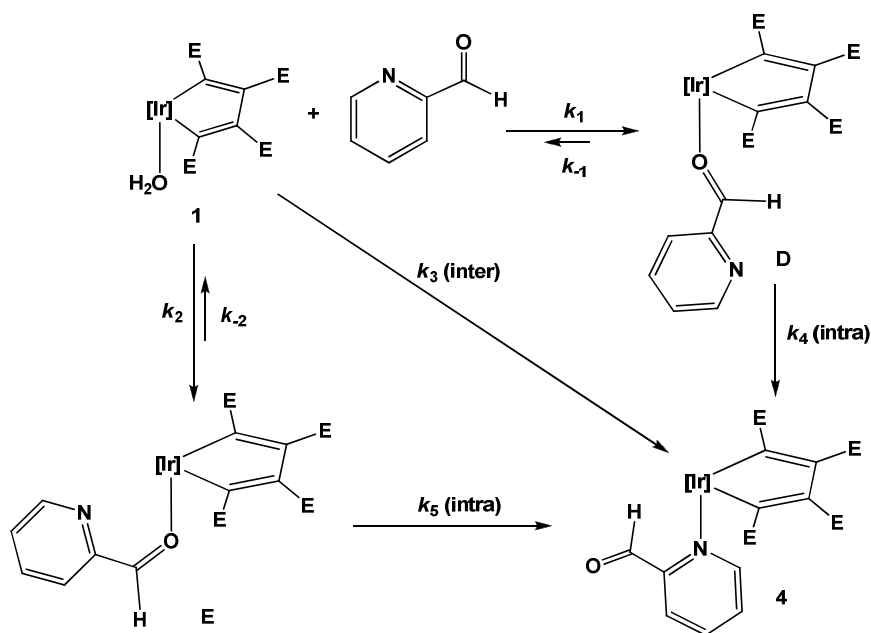


Figure 5. X-ray structure of compound **4** (50% displacement ellipsoids, H atoms except the H atom on C(26) omitted for clarity). Selected bond lengths (Å) and angles (deg): Ir(1)—C(10) 2.021(3), Ir(1)—C(1) 2.030(3), C(7)—C(10) 1.366(4), C(1)—C(4) 1.364(4), Ir(1)—N(1) 2.105(3), Ir(1)—N(2) 2.066(2), Ir(1)—N(4) 2.132(2), Ir(1)—N(6) 2.162(3); C(1)—Ir(1)—C(10) 78.92(12).

Two transient "intermediate" aldehydic *O*-adducts, species **D** and **E** characterized by $\text{ArC(=O)H}^1\text{H}$ NMR signals at 10.41 and 10.22 ppm respectively (vs. 9.92 ppm for the free ligand), are formed on route to **4** (Scheme 5). These were observed when the reaction of complex **1** and 2-pyridinecarboxaldehyde

was monitored in CD_2Cl_2 at 25 °C, under pseudo first-order conditions. The first *O*-adduct to appear was **D**, having a structure related to compounds **3** and thereafter, **E** and the final product **4** began to appear, long before the starting material **1** was completely consumed. Although no quantitative kinetic analysis has been carried out, qualitative observations are in accord with the transformations shown in Scheme 5 with $k_1 > k_2$ and k_3, k_5 being slightly larger than k_4 (or k_2 being slightly larger than k_1 if the formation of **4** is strictly intermolecular *i.e.* through k_3).

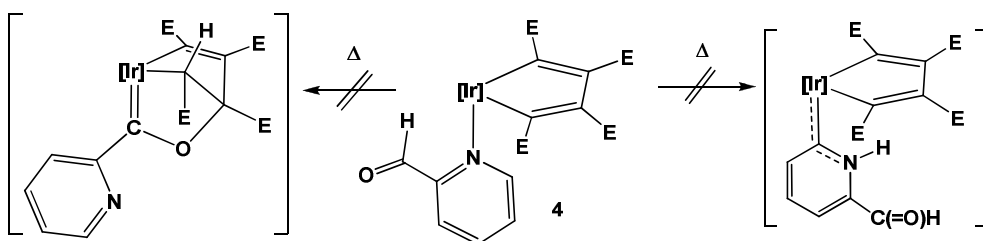


Scheme 5. The reaction products observed in the reaction of **1** with 5 equiv. of 2-pyridinecarboxaldehyde (CD_2Cl_2 , 25 °C).

The structure proposed for **E** is based on the high field shifts of the protons of the pyridyl residue in the ^1H NMR spectrum. Clearly, **D** and **E** can not interconvert *via* a simple rotation around the $\text{Ir}-\text{O}$ bond and therefore this process has to take place intermolecularly, *i.e.* by extrusion and addition of the aldehyde ligand. As no species related to **E** are observed in any other case, we propose that the stabilization of this structure for this particular aldehyde may be due to a favourable π -stacking of the pyridyl and pyrazolyl aromatic rings.

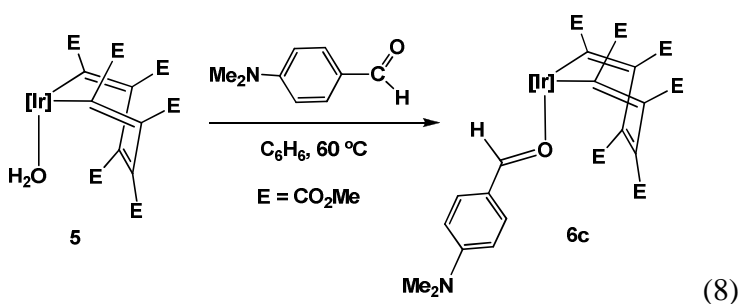
An interesting type of behaviour was observed by ^1H NMR spectroscopy just after **1** and excess of 2-pyridinecarboxaldehyde were mixed, at 25 °C in CD_2Cl_2 , and before any species of Scheme 5 began to appear. The Tp^{Me_2} resonances of **1**, while maintaining the 2:1 symmetry, were replaced by new ones, but no additional aldehydic or pyridyl signals appeared. In due time and as commented above, the system evolved as shown in Scheme 5. As this phenomena is only restricted to this particular aldehyde, and because a similar behaviour occurs when **1** reacts with pyridine, *i.e.* before formation of the *N*-adduct $\text{Tp}^{\text{Me}_2}\text{Ir}[\text{C}(\text{CO}_2\text{Me})=\text{C}(\text{CO}_2\text{Me})\text{C}(\text{CO}_2\text{Me})=\text{C}(\text{CO}_2\text{Me})](\text{NC}_5\text{H}_5) \mathbf{1}\cdot(\text{NC}_5\text{H}_5)^{14\text{b}}$ is observed, we conclude that both pyridine substrates interact with **1** forming corresponding labile second-sphere coordination species (so-called loosely complexes²⁰), with the pyridine ring being fundamental for their formation.

Compound **4** is a quite stable species and neither carbene formation of the type reported in this paper nor tautomerization of the pyridine take place in C_6H_6 solution at 120-150 °C (Scheme 6). The latter transformation occurs when complex **1** and other $\text{Tp}^{\text{Me}_2}\text{Ir}(\text{III})(\text{R})(\text{R}')(\text{L})$ species ($\text{R}, \text{R}' = \text{alkyl, aryl}; \text{L} = \text{labile ligand}$) react with a variety of 2-substituted pyridines under milder conditions.^{19,21} In fact, DFT calculations show that the tautomerized carbene is *ca.* 2 $\text{kcal}\cdot\text{mol}^{-1}$ more stable than the *N*-adduct while the carbene of the type described in this paper is even more stable by *ca.* 8 $\text{kcal}\cdot\text{mol}^{-1}$. That these unobserved transformations are not due to the lack of lability of the $\text{Ir}\leftarrow\text{N}$ bond is clearly supported by the exchange reaction of **4** that takes place with pyridine to give the adduct $\text{Tp}^{\text{Me}_2}\text{Ir}[\text{C}(\text{CO}_2\text{Me})=\text{C}(\text{CO}_2\text{Me})\text{C}(\text{CO}_2\text{Me})=\text{C}(\text{CO}_2\text{Me})](\text{NC}_5\text{H}_5)$ commented above (90 °C, $t_{1/2} = 16$ h). Interestingly, compound **4** decomposes instead, in C_6H_6 at 150 °C, with formation of the carbonyl derivative $\mathbf{1}\cdot\text{CO}$ depicted in Scheme 3 of the Introduction (*ca.* 80% NMR spectroscopic yield). Why this particular aldehyde experiences an almost clean decarbonylation, not the case for other aromatic aldehydes studied in this paper (*i.e.* benzaldehyde and its *p*- NO_2 derivative, see above), is something that we cannot explain so far.



Scheme 6. Structures of the carbenes expected from complex **4** on the basis of the results obtained in this paper (left) and in reference 21 (right).

The formation of *O*-aldehyde adducts described in eq 6 is general for a wider variety of iridacycles. Thus, we have studied their formation from the aquoiridacycloheptatriene **5**²² and eq 8 shows the result of the reaction of this complex with *p*-dimethylaminobenzaldehyde. The new derivative **6c** is easily characterized by NMR; the six CO₂Me groups of the metallacycle give rise to only 3 signals (6 H each). This shows that the molecule keeps the symmetry plane of the starting material after the exchange water-aldehyde has taken place. The chemical shift of the aldehyde H atom (8.16 ppm) indicates a different chemical environment for this nucleus when compared with compound **3c** (9.50 ppm), and it is probable that the presence of the 7-membered metallacycle, which adopts a boat conformation,²³ forces the coordinated aldehyde to adopt the rotameric conformation shown in eq 8, in which the pyrazolyl rings shield this proton.



This rotamer is also the preferred one in the solid state and Figure 6 shows an ORTEP view of the molecules of this compound, along with some selected bond distances and angles. As can be observed, the metallacycle features a boat structure with the central C=C bond pointing towards the metal centre as previously observed in related species^{22,23} The aldehyde ligand is coordinated to the iridium atom by the

oxygen atom and the Ir—O(1) bond distance is a normal one of 2.090(2) Å. Also, the two Ir—C(sp²) bond lengths exhibit values in the expected range (2.044(4) and 2.049(4) Å).

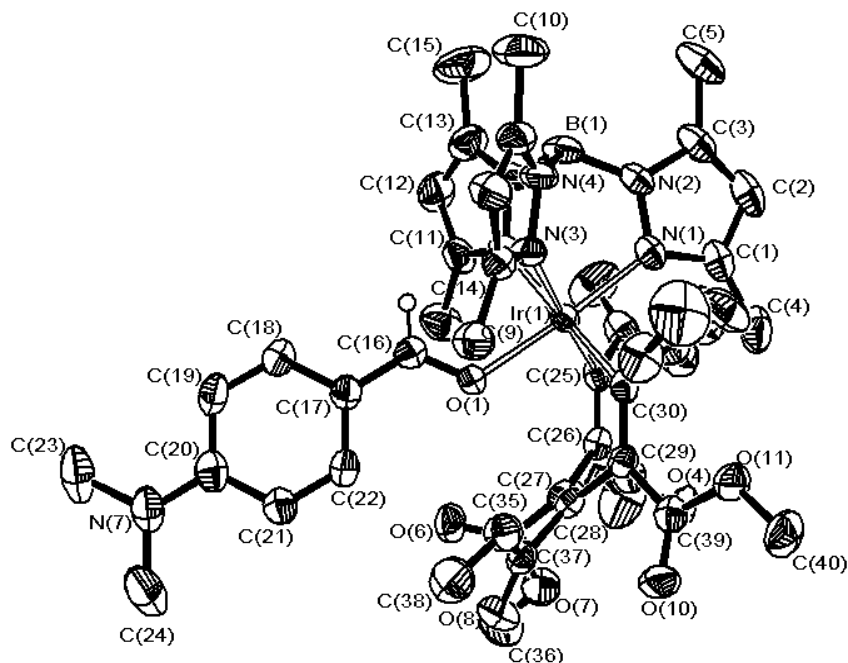


Figure 6. X-ray structure of compound **6c** (50% displacement ellipsoids, H atoms except the H atom on C(16) omitted for clarity). Selected bond lengths (Å) and angles (deg): Ir(1)—N(1) 2.036(3), Ir(1)—N(5) 2.128(3), Ir(1)—N(3) 2.133(3), Ir(1)—C(30) 2.044(4), Ir(1)—C(25) 2.049(4), Ir(1)—O(1) 2.090(2); C(30)—Ir(1)—C(25) 90.69(16), C(30)—Ir(1)—O(1) 91.29(13), C(25)—Ir(1)—O(1) 94.91(13).

Another *O*-adduct **6g**, is formed upon the reaction of complex **5** and 2-pyrrolicarboxaldehyde (eq 9). NMR data once more support the solution structure depicted in eq 9 and it has also been confirmed in the solid state by an X-ray structure determination. Figure 7 shows an ORTEP representation of the molecule, along with some selected bond distances and angles. Because of the similarity of complexes **6c** and **6g**, no further discussion is required, although the presence of a hydrogen bond between the pyrrol NH group and one of the CO₂Me oxygen atoms, O(8), can be of some interest.

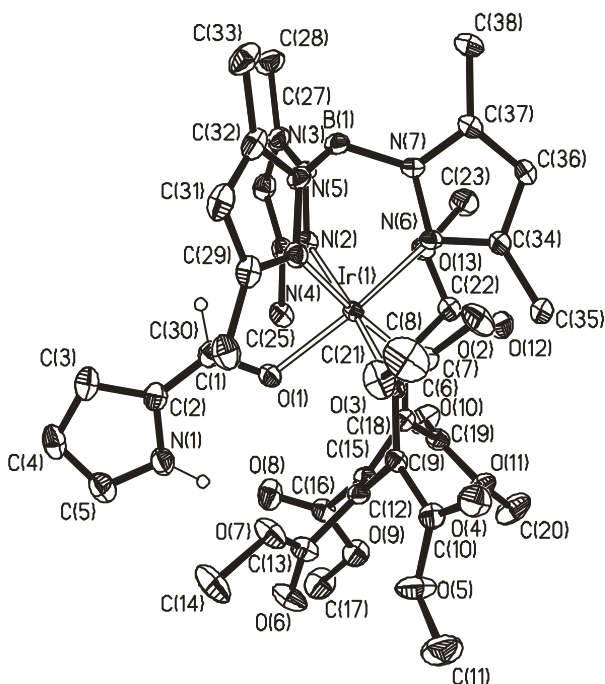
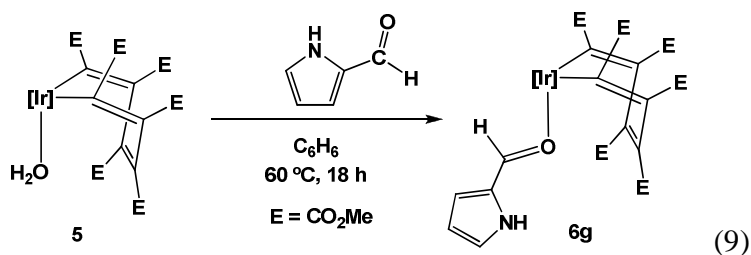


Figure 7. X-ray structure of compound **6g** (50% displacement ellipsoids, H atoms except the H atoms on C(1) and N(1) omitted for clarity). Selected bond lengths (Å) and angles (deg): Ir(1)—N(2) 2.120(2), Ir(1)—N(4) 2.136(2), Ir(1)—N(6) 2.036(2), Ir(1)—C(6) 2.029(3), Ir(1)—C(21) 2.041(3), Ir(1)—O(1) 2.0824(19); C(6)—C(9) 1.366(4), C(9)—C(12) 1.486(4), C(12)—C(15) 1.340(4), C(15)—C(18) 1.482(4), C(18)—C(21) 1.349(4); C(6)—Ir(1)—C(21) 90.21(10), O(1)—Ir(1)—C(6) 91.65(9), O(1)—Ir(1)—C(21) 93.58(9).

Finally and not unexpectedly in view of the structures of compounds **6c** and **6g**, these compounds do not transfer the aldehydic H atom to the β -carbon of the metallacycle even when heated at 120 °C for prolonged periods of time. Note that in the case of adducts **3**, the aldehydic H atom always points

towards the metallacycle, and this probably facilitates the transfer to one of the double bonds; in the case of compounds **6c** and **6g**, these H atoms are located far from the metallacycle and the required rotameric conformation is probably too crowded to be accessible.

DFT calculated mechanism for the formation of bicyclic Fisher carbenes.

In a recent paper on the reactivity of complex **1** towards aliphatic aldehydes¹² we proposed a DFT-based mechanism for the observed decarbonylations, in which aldehyde C—H activation with H migration to a α -carbon of the iridacycle, followed by H back-migration onto the alkyl fragment of the resulting acyl ligand were the key steps in the reaction (Scheme 3). In this paper we report a related study to justify why in this case aliphatic aldehydes yield the bicyclic carbene complexes **2** instead of the expected decarbonylation product. This study uses benzaldehyde and a metallic model systems, in which the CO₂Me fragments of the iridacycle unit of **1** were replaced by hydrogen atoms. QM:MM methods (ONIOM) were used to model the Tp^{Me2} ligand with the methyl fragments calculated at the molecular mechanics (Uff) level and the rest of the molecule at the QM level. Figure 8 shows the potential energy profiles for the formation of bicyclic carbenes and the unobserved decarbonylation reaction. Both reactions start by water substitution in **1** to yield the benzaldehyde *O*-adduct **3_C**, which has been chosen as the potential energy origin. The calculations indicate that this step is endoergic by less than 1.5 kcal·mol⁻¹ in the gas phase, which is consistent with the isolation of the *O*-adducts **3**. The next step, C—H activation of benzaldehyde by the metallic fragment, requires formation of an unstable σ -H complex (**F_C**), and the overall barrier for C—H activation from **3_C** amounts 32.0 kcal·mol⁻¹. When the less sterically demanding Tp ligand was used in the calculations instead of Tp^{Me2}, the only significant difference in the energy profile was the energy barrier for this step, which now is lower at 27.4 kcal·mol⁻¹. This step gives an acyl intermediate (**G_C**) which can either undergo decarbonylation or C—O coupling to form the bicyclic carbene. In the first case, H back migration from the iridacycle onto the C₆H₅ moiety of the acyl ligand has a high energy barrier (in excess of 40 kcal·mol⁻¹). The second pathway requires rotation of the acyl ligand about the Ir—C bond to place the O atom of the aldehyde pointing towards

the metallacycle ring. This rotation has a moderate barrier of $10.8 \text{ kcal}\cdot\text{mol}^{-1}$ from \mathbf{G}_C to give the corresponding rotamer \mathbf{G}'_C , which is more stable than the former by $3.6 \text{ kcal}\cdot\text{mol}^{-1}$. The last step in this pathway, C—O coupling to give the bicyclic carbene \mathbf{C}_C is almost barrier-less and the overall reaction is exothermic by $10.8 \text{ kcal}\cdot\text{mol}^{-1}$. As already discussed the resulting species \mathbf{C}_C is the product of the *syn* H addition, while the *anti* stereoisomers (**2**) are isolated. Full QM calculations on the real system show that formation of **2a** vs. the corresponding *syn* stereoisomer is thermodynamically favorable by *ca.* $7 \text{ kcal}\cdot\text{mol}^{-1}$.

The results of this study suggest that formation of the bicyclic carbenes is kinetically preferred to decarbonylation. Despite the former is reversible, the latter may be prevented in the case of aromatic aldehydes by the high energy barrier required for H back migration from the metallacycle to the aryl moiety of the acyl intermediates (\mathbf{G}_C).

It should be said that in our previous work¹² the calculated barrier for decarbonylation of acetaldehyde was almost identical to the reported here for benzaldehyde, while in the case of aliphatic aldehydes the expected decarbonylation reactions were observed. Theoretical results at this level of theory (and with the use of model molecules) can be expected to qualitatively agree with experimental results, and although in this case we cannot justify the absence of decarbonylation in reactions with aromatic aldehydes, a few $\text{kcal}\cdot\text{mol}^{-1}$ difference in the overall experimental energy barriers would be enough to explain the different reactivity.

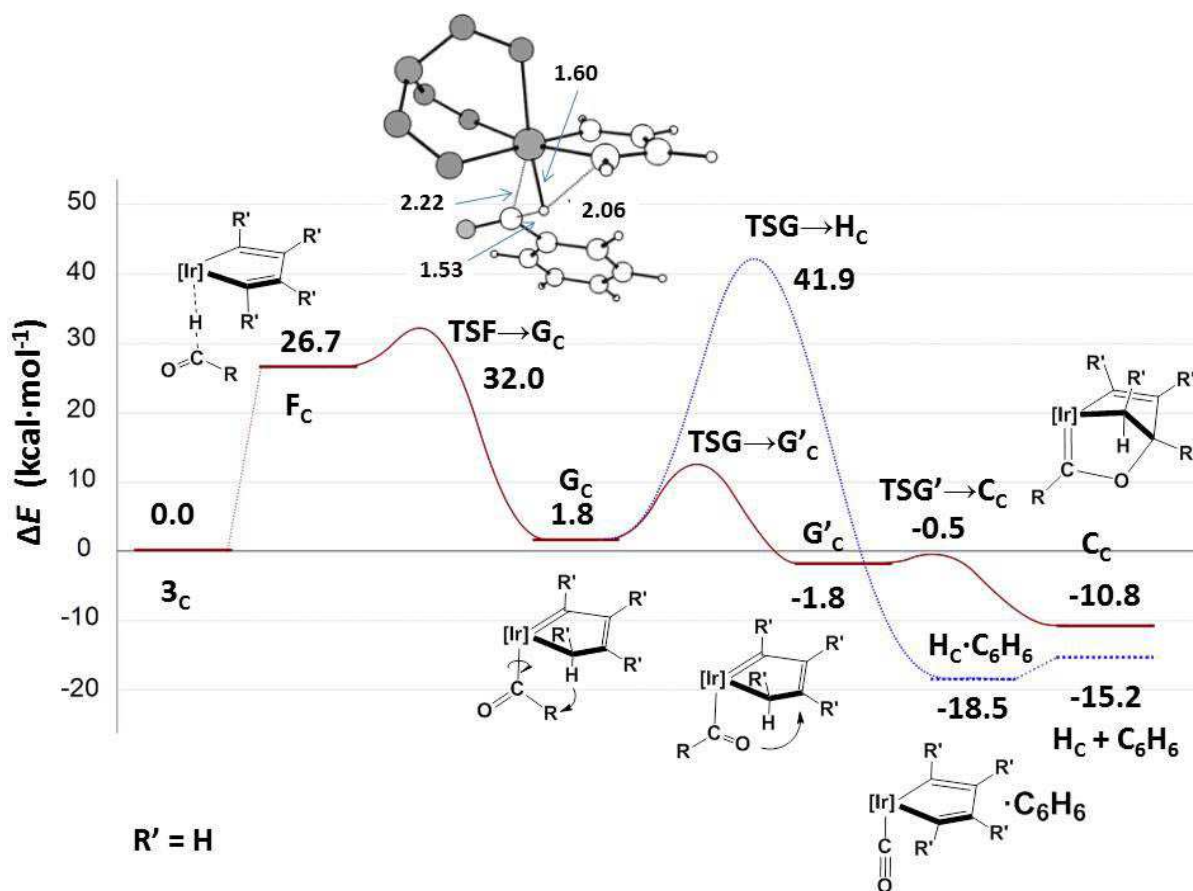


Figure 8. Calculated potential energy profiles for the formation of the bicyclic Fischer carbene **C** (red solid line) and the decarbonylation of benzaldehyde (blue dotted line). The inset shows the calculated transition state for benzaldehyde C—H activation (C and H atoms of the Tp^{Me_2} ligand have been omitted for clarity).

CONCLUDING REMARKS

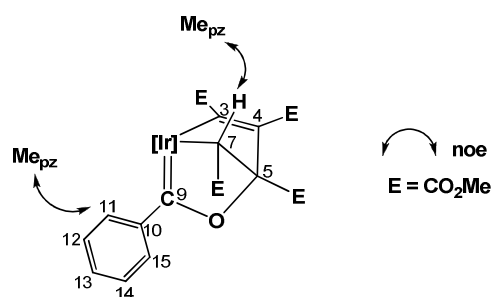
Three different iridacyclopentadienes, **1**, **1(C₆H₄)** and **1(H)**, react with aromatic aldehydes forming initially, at 25-60 °C, the *O*-adducts **3**, which under more forcing conditions (90-120 °C) transform into the bicyclic Fischer carbenes **2**. These findings strongly contrast with the reactions of **1** with aliphatic aldehydes which, at 120 °C and through *O*-adduct intermediates, lead to the Ir-carbonyl adduct **1•CO** and the corresponding alkane. In the latter case no bicyclic Fischer carbenes have been observed while no similar decarbonylation process takes place for the aromatic cases. Surprisingly, 2-

pyridinecarboxaldehyde behaves quite differently, forming a very stable *N*-adduct which eventually yields the carbonyl derivative of Scheme 3 under forcing conditions (150 °C).

EXPERIMENTAL SECTION

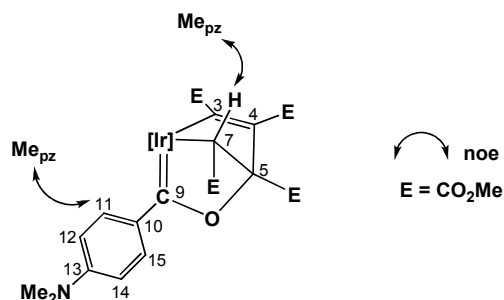
General considerations. All the manipulations were carried out under an inert atmosphere, following Schlenk techniques. The solvents employed were dried before use. The elemental analyses of the new compounds were carried out at the Microanalytical Service of the Instituto de Investigaciones Químicas (Sevilla) (Perkin Elmer Serie II CHNS/O 2400). IR spectra were recorded at Perkin-Elmer system 2000 FT-IR (KBr). NMR instruments were Bruker modes DPX-300, DRX-400 and DRX-500. ^1H and ^{13}C resonances were referenced with respect to SiMe_4 using the residual protio solvent peaks as internal standard (^1H NMR) and the characteristic resonances of the solvent ^{13}C nuclei (^{13}C NMR). Most of ^1H and ^{13}C assignments were based in mono and bidimensional experiments ($^{13}\text{C}\{^1\text{H}\}$ -gated, COSY, NOESY, ^1H - ^{13}C HMQC and HMBC). For a series of very similar compounds, only some of them were analyzed or investigated by NMR in full. Compounds **1**, **1**(C_6H_4), **1**(**H**), and **5** were prepared by the procedures described in the literature.

Synthesis of the benzaldehyde derivative 2a. To a stirred suspension of compound **1** (0.100 g, 0.126 mmol) in C_6H_6 (3 mL), freshly distilled benzaldehyde (38.4 μl , 0.37 mmol) was added and the mixture was stirred for 12 h at 120 °C. After this period of time, the solvent was evaporated under vacuo, and the residue was subjected to column chromatography (silica gel) with a mixture of diethyl ether:hexane (10:90) as eluent. Yield: 0.08 g, *ca.* 70% yield. From a diethyl ether solution of this solid, a yellow crystalline sample of analytical purity was obtained by cooling at -20 °C.



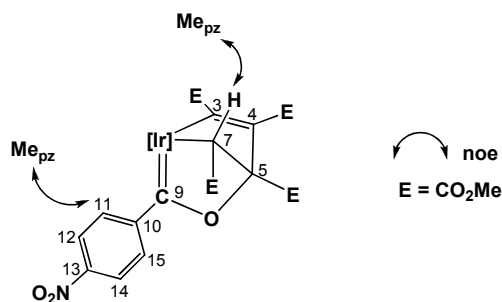
be located. Anal. Calcd. for $C_{35}H_{42}BN_6O_{10}Ir$: C, 46.20, H, 4.65, N, 9.24. Found: C, 46.22, H, 4.43, N, 9.11. IR (KBr) ν (cm^{-1}): (Me) 2953, 2850, (BH) 2530, (CO₂Me) 1712.

Synthesis of carbene 2c. Following the above procedure but employing *p*-dimethylaminobenzaldehyde, compound **2c** was obtained as a yellow solid in *ca.* 55% yield.



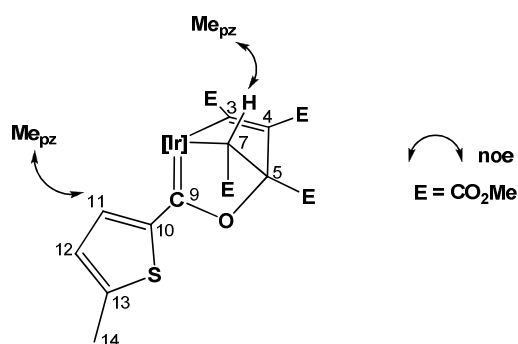
1H NMR ($CDCl_3$, 25 °C): δ (ppm) 8.24 (dd, 1 H, $^3J_{H-H} = 9.1$, $J_{H-H} = 2.2$ Hz, CH₁₅), 6.65 (dd, 1 H, $^3J_{H-H} = 9.1$, $J_{H-H} = 2.2$ Hz, CH₁₁), 6.41 (dd, 1 H, $^3J_{H-H} = 9.1$, $J_{H-H} = 2.2$ Hz, CH₁₄), 6.01 (dd, 1 H, $^3J_{H-H} = 9.1$, $J_{H-H} = 2.2$ Hz, CH₁₂), 5.81, 5.60, 5.59 (s, 1 H each CH_{pz}), 5.08 (s, 1 H, H₇), 3.76, 3.64, 3.25, 3.22 (s, the first broad, 3 H each, CO₂Me), 2.93 (s, 6 H, NMe₂), 2.46, 2.42, 2.39, 1.38, 1.16 (s, 1:1:2:1:1, 18 H, Me_{pz}). $^{13}C\{^1H\}$ NMR ($CDCl_3$, 25 °C): δ (ppm) 242.7 (C₉), 182.0, 174.0, 162.6 (CO₂Me), 154.7, 152.6, 151.3, 144.2, 143.4, 143.2 (C_{qpz}), 154.5 (C₁₃), 139.5 (C₁₁), 133.2 (C₁₀), 128.6 (C₁₅), 110.5 (C₁₂), 110.0 (C₁₄), 108.6, 107.1, 106.5 (CH_{pz}), 108.2 (C₅), 52.7, 51.9, 50.9, 50.7 (the first broad, CO₂Me), 40.3 (NMe₂), 33.2 (C₇, $^1J_{C-H} = 137$ Hz), 16.2, 15.9, 14.7, 13.5, 13.2, 13.2 (Me_{pz}). C₃ and C₄ and one of the CO₂Me are too weak to be located. IR (KBr) ν (cm^{-1}): (Me) 2923, 2853, (BH) 2527, (CO₂Me) 1720.

Synthesis of carbene 2d. This derivative can be prepared following the same procedure than for the previous carbenes, but employing *p*-nitrobenzaldehyde.



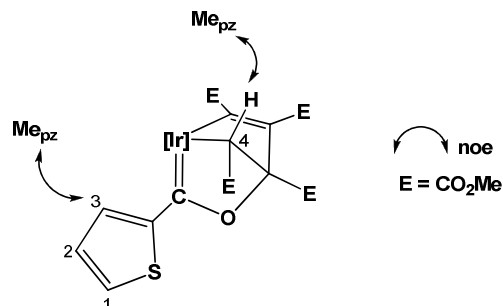
^1H NMR (CDCl_3 , 25 °C): δ (ppm) 8.46 (d, 1 H, $^3J_{\text{H-H}} = 8.0$ Hz, H_{15}), 8.11 (d, 1 H, $^3J_{\text{H-H}} = 8.0$ Hz, H_{14}), 7.71 (d, 1 H, $^3J_{\text{H-H}} = 8.0$ Hz, H_{12}), 7.12 (d, 1 H, $^3J_{\text{H-H}} = 8.0$ Hz, H_{11}), 5.87, 5.69, 5.62 (s, 1 H each, CH_{pz}), 5.38 (s, 1 H, H_7), 3.97, 3.68, 3.26, 3.24 (s, the first broad, 3 H each, CO_2Me), 2.49, 2.46, 2.45, 2.44, 1.34, 0.91 (s, 3 H each, Me_{pz}). $^{13}\text{C}\{^1\text{H}\}$ NMR (CDCl_3 , 25 °C): δ (ppm) 251.3 (C_9), 180.7, 172.5, 170.6, 161.7 (CO_2Me), 154.8, 151.7, 149.9, 144.8, 144.0, 143.8 (C_{qpz}), 147.7 (C_{10}), 136.2 (C_{11}), 126.1 (C_{15}), 123.4 (C_{14}), 123.0 (C_{12}), 108.7, 107.2, 106.7 (CH_{pz}), 106.8 (C_5), 52.6, 51.8, 50.8, 50.6 (the first broad, CO_2Me), 34.0 (C_7), 15.8, 15.4, 14.8, 13.1, 12.9, 12.7 (Me_{pz}). C_3 and C_4 are too weak to be located.

Synthesis of carbene 2e. This derivative can be prepared following the same procedure than for the previous carbenes, but employing 5-methyl-2-thiophenecarboxaldehyde. **2e** was isolated as an orange solid in *ca.* 75% yield. In this case, the eluent was a mixture of diethyl ether:hexane (50:50).



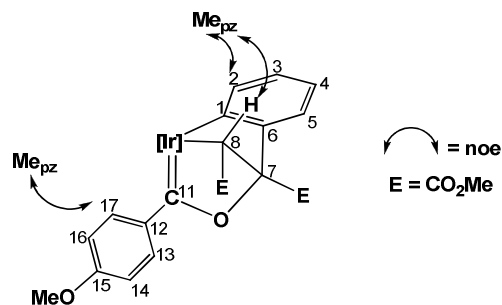
^1H NMR (CDCl_3 , 25 °C): δ (ppm) 6.47 (d, 1 H, $^3J_{\text{H-H}} = 3.9$ Hz, CH_{11}), 6.42 (d, 1 H, $^3J_{\text{H-H}} = 3.9$ Hz, CH_{12}), 5.84, 5.64, 5.62 (s, 1 H each, CH_{pz}), 5.17 (s, 1 H, H_7), 3.94, 3.66, 3.28, 3.25 (s, the first broad, 3 H each, CO_2Me), 2.47, 2.44, 2.41, 2.40, 1.39, 1.24 (s, 3 H each, Me_{pz}), 2.32 (s, 3 H, Me_{14}). $^{13}\text{C}\{^1\text{H}\}$ NMR (CDCl_3 , 25 °C): δ (ppm) 235.7 (C_9), 181.3, 173.5, 169.7, 161.9 (CO_2Me), 154.5, 151.9, 150.5, 143.9, 143.2, 143.2 (C_{qpz}), 152.8 (C_{13}), 145.7 (C_{10}), 143.3 (C_{11}), 143.2 (C_5), 128.1 (C_{12}), 108.3, 106.9, 106.4 (CH_{pz}), 107.2 (C_5), 52.4, 51.5, 50.6, 50.4 (the first broad, CO_2Me), 33.3 (C_7), 16.2 (Me_{14}), 15.7, 15.8, 14.2, 13.0, 12.8, 12.6 (Me_{pz}). C_3 and C_4 are too weak to be located. Anal. Calcd. for $\text{C}_{33}\text{H}_{40}\text{BIrN}_6\text{O}_9\text{S}$: C, 44.05, H, 4.48, N, 9.34, S, 3.56. Found: C, 44.17, H, 4.68, N, 9.22, S, 3.52. IR (KBr) ν (cm^{-1}): (Me) 2947, (BH) 2532, (CO_2Me) 1726, 1711.

Synthesis of carbene 2f. The procedure described for **2a**, but using 2-thiophenecarboxaldehyde, produced compound **2f** as an orange solid in *ca.* 45% yield. The solvent used for column chromatography was diethyl ether:hexane (50:50).



^1H NMR (CDCl_3 , 25 °C): δ (ppm) 7.75 (d, 1 H, $^3J_{\text{H-H}} = 4.3$ Hz, H_3), 6.71 (t, 1 H, $^3J_{\text{H-H}} = 4.3$ Hz, H_2), 6.66 (d, 1 H, $^3J_{\text{H-H}} = 4.3$ Hz, H_1), 5.84, 5.64, 5.62, (s, 1 H each, CH_{pz}), 5.21 (s, 1 H, H_4), 3.93, 3.66, 3.27, 3.24 (s, the first broad, 3 H each, CO_2Me), 2.47, 2.43, 2.41, 2.40, 1.35, 1.22 (s, 3 H each, Me_{pz}).

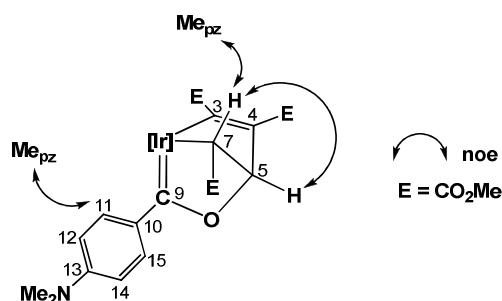
Synthesis of carbene 2(C₆H₄)b. Following the procedure described for **2b** but starting from metallacycle **1(C₆H₄)** (0.100 g, 0.12 mmol) in C_6H_{12} (3 mL) and anisaldehyde (43.8 μl , 0.36 mmol), the title compound could be obtained, as a yellow material after column chromatography on silica gel using a 50:50 mixture of diethyl ether:hexane as eluent. Yield: *ca.* 75%.



^1H NMR (CDCl_3 , 25 °C): δ (ppm) 8.17 (dd, 1 H, $^3J_{\text{H-H}} = 8.8$, $J_{\text{H-H}} = 2.3$ Hz, H_{13}), 7.09 (d, 1 H, $^3J_{\text{H-H}} = 7.3$, H_5), 6.98 (dd, 1 H, $^3J_{\text{H-H}} = 8.8$, $J_{\text{H-H}} = 2.2$ Hz, H_{17}), 6.91 (td, 1 H, $^3J_{\text{H-H}} = 7.2$, $J_{\text{H-H}} = 1.5$ Hz, H_4), 6.75 (td, 1 H, $^3J_{\text{H-H}} = 7.3$, $J_{\text{H-H}} = 1.3$ Hz, H_3), 6.71 (dd, 1 H, $^3J_{\text{H-H}} = 7.3$, $J_{\text{H-H}} = 1.3$ Hz, H_2), 6.66 (dd, 1 H, $^3J_{\text{H-H}} = 8.8$, $J_{\text{H-H}} = 2.6$ Hz, H_{14}), 6.34 (dd, 1 H, $^3J_{\text{H-H}} = 8.8$, $J_{\text{H-H}} = 2.6$ Hz, H_{16}), 5.72, 5.69, 5.64 (s, 1 H each, CH_{pz}), 4.99 (s, 1 H, H_8), 4.04 (s, 3 H, CO_2Me), 3.71 (s, 3 H, OMe), 3.28 (s, 3 H, CO_2Me), 2.48, 2.47, 2.45, 1.54, 1.46, 0.78 (s, 3 H each, Me_{pz}). $^{13}\text{C}\{^1\text{H}\}$ NMR (CDCl_3 , 25 °C): δ (ppm) 247.4 (C_{11}), 182.5,

170.8 (CO₂Me), 163.7 (C₁₅), 152.6, 151.9, 149.8, 143.9, 143.2, 143.2 (C_{qpz}), 146.9 (C₆), 141.3 (C₁), 138.6 (C₁₇), 138.3 (C₁₂), 136.2 (C₂), 126.8 (C₁₃), 125.8 (C₃), 122.0 (C₄), 120.0 (C₅), 113.3 (C₁₆), 112.8 (C₁₄), 108.3, 106.6, 106.6 (CH_{pz}), 106.8 (C₇), 55.2 (OMe), 52.2, 50.3 (CO₂Me), 33.0 (C₈), 14.7, 14.2, 13.8, 13.1, 12.8, 12.7 (Me_{pz}). Anal. Calcd. for C₃₅H₄₀BN₆O₆Ir: C, 46.20, H, 4.65, N, 9.24. Found: C, 49.82, H, 4.89, N, 10.03. IR (KBr) ν (cm⁻¹): (Me) 2923, (BH) 2526, (CO₂Me) 1705.

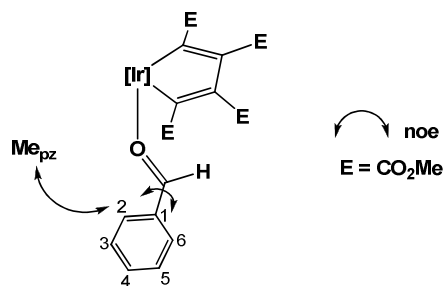
Synthesis of carbene 2(H)c. Following the procedure described for carbene **2c**, but starting from **1(H)**, the title compound was isolated in *ca.* 60% yield, by washing the residue obtained after evaporation of the solvent with a cold mixture (1:1) of diethyl ether:hexane.



¹H NMR (CDCl₃ 25 °C): δ (ppm) 8.01 (dd, 1 H, ³J_{H-H} = 9.1, J_{H-H} = 2.2 Hz, H₁₅), 6.61 (dd, 1 H, ³J_{H-H} = 9.1, J_{H-H} = 2.2 Hz, H₁₁), 6.59 (s, 1 H, H₅), 6.40 (dd, 1 H, ³J_{H-H} = 9.1, J_{H-H} = 2.2 Hz, H₁₄), 6.00 (dd, 1 H, ³J_{H-H} = 9.1, ¹J_{H-H} = 2.2 Hz, H₁₂), 5.80, 5.61, 5.60 (s, 1 H each, CH_{pz}), 4.58 (s, 1 H, H₇), 3.72, 3.34, 3.28 (s, 1 H each, CO₂Me), 2.98 (s, 6 H, NMe₂), 2.42, 2.41, 2.40, 2.39, 1.39, 1.17 (s, 3 H each, Me_{pz}).

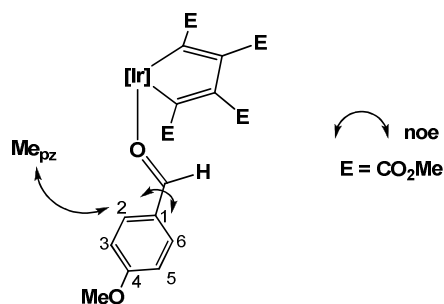
¹³C{¹H} NMR (CDCl₃, 25 °C): δ (ppm) 246.2 (C₉), 182.8, 174.6, 162.4 (CO₂Me), 166.0 (C₃ or C₄), 154.1, 152.1, 151.1, 143.7, 142.9, 142.9 (C_{qpz}), 153.7 (C₁₃), 138.8 (C₁₁), 137.7 (C₄ or C₃), 132.9 (C₁₀), 127.1 (C₁₅), 110.0 (C₁₂), 109.5 (H₁₄), 108.1, 106.6, 106.0 (CH_{pz}), 98.9 (C₅, ¹J_{C-H} = 160 Hz), 51.3, 50.6, 50.3 (CO₂Me), 39.8 (NMe₂), 28.6 (C₇, ¹J_{C-H} = 134 Hz), 15.9, 15.7, 14.1, 13.1, 12.9, 12.8 (Me_{pz}).

Synthesis of adduct 3a. Compound **1** (0.100 g, 0.126 mmol) was dissolved in dichloromethane (3 mL) and benzaldehyde (12.5 μ l, 0.13 mmol) was added. The mixture was stirred for 6 h at 60 °C, the solvent was eliminated under vacuo, and the residue was washed twice with cold (0 °C) hexane to yield the title compound, as a red solid, in *ca.* 90% yield. Due to the reversible formation of **1** in the presence of adventitious water, this and other of the adducts could not be completely purified.



^1H NMR (CDCl_3 , 25 °C): δ (ppm) 10.22 (s, 1 H, C(O)H), 7.86 (d, 2 H, $^3J_{\text{H-H}} = 7.5$ Hz, H₂, H₆), 7.68 (t, 1 H, $^3J_{\text{H-H}} = 7.5$ Hz, H₄), 7.43 (d, 2 H, $^3J_{\text{H-H}} = 7.5$ Hz, H₃, H₅), 5.73, 5.56 (s, 2:1, 3 H, CH_{pz}), 3.78, 3.34 (s, 6 H each, CO₂Me), 2.42, 2.39, 2.09, 1.71 (s, 1:2:1:2, 18 H, Me_{pz}). $^{13}\text{C}\{^1\text{H}\}$ NMR (CDCl_3 , 25 °C): δ (ppm) 205.3 (C(O)H), 173.3, 166.9 (1:1, CO₂Me), 156.0, 150.3, 143.6, 143.5 (1:2:2:1, C_{qpz}), 150.4, 143.4 (1:1, CCO₂Me), 136.9 (C₄), 134.1 (C₁), 131.6 (C₂, C₆), 129.5 (C₃, C₅), 108.0, 106.7 (2:1, CH_{pz}), 51.8, 50.8 (1:1, CO₂Me), 13.4, 13.3, 12.9, 12.5 (2:1:1:2, Me_{pz}).

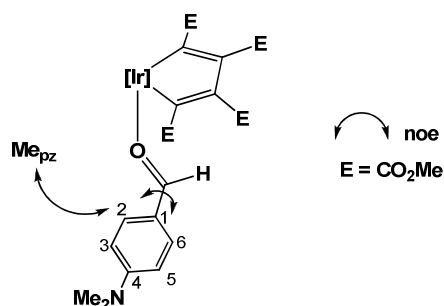
Synthesis of complex 3b. To a solution of complex **1** (0.100 g, 0.126 mmol) in CH_2Cl_2 (3 mL), *p*-anisaldehyde was added (46 μl , 0.37 mmol). The mixture was stirred at 60 °C for 6 h, the solvent was evaporated under vacuo, and the remaining residue was purified by silica gel column chromatography (hexane:diethyl ether, 20:80). The analytical sample was crystallized from diethyl ether, at -20 °C, as orange crystals (0.069 g, *ca.* 60% yield).



^1H NMR (CDCl_3 , 25 °C): δ (ppm) 9.92 (s, 1 H, C(O)H), 7.82 (d, 2 H, $^3J_{\text{H-H}} = 8.4$ Hz, H₂, H₆), 6.89 (d, 2 H, $^3J_{\text{H-H}} = 8.7$ Hz, H₃, H₅), 5.55, 5.72 (s, 2:1, 3 H, CH_{pz}), 3.80 (s, 3 H, OMe), 3.77, 3.34 (s, 6 H each, CO₂Me), 2.41, 2.39, 2.08, 1.72 (s, 1:2:1:2, 18 H, Me_{pz}). $^{13}\text{C}\{^1\text{H}\}$ NMR (CDCl_3 , 25 °C): δ (ppm) 201.6 (C(O)H), 173.5, 166.9 (1:1, CO₂Me), 166.8 (C₄), 155.9, 150.5, 143.5, 143.4 (1:2:2:1, C_{qpz}), 158.0, 150.1 (1:1, CCO₂Me), 135.4 (C₂, C₆), 127.6 (C₁), 115.0 (C₃, C₅), 108.1, 106.7 (2:1, CH_{pz}), 55.9 (OMe), 51.7,

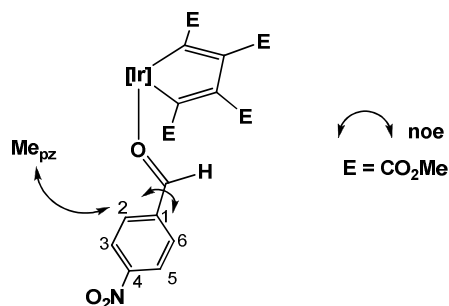
50.8 (1:1, CO₂Me), 13.4, 13.4, 12.9, 12.6 (2:1:1:2, Me_{pz}). Anal. Calcd. for C₃₅H₄₂BN₆O₁₀Ir: C, 46.20, H, 4.65, N, 9.24. Found: C, 46.20, H, 4.66, N, 9.47. IR (KBr) ν (cm⁻¹): (Me) 2942, (BH) 2529, (CO₂Me) 1733, 1717, 1706.

Synthesis of adduct 3c. Following the procedure used for **3b** but using *p*-dimethylaminobenzaldehyde, a crude material was obtained, which, after being washed with cold diethyl ether, yielded **3c** as a red solid in *ca.* 70% yield.



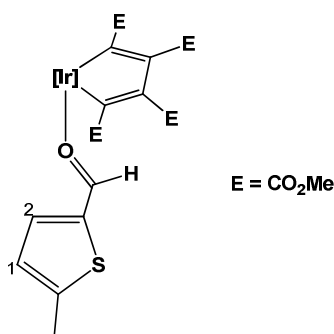
¹H NMR (CDCl₃, 25 °C): δ (ppm) 9.50 (s, 1 H, C(O)H), 7.65 (d, 2 H, ³J_{H-H} = 8.7 Hz, H₂, H₆), 6.55 (d, 2 H, ³J_{H-H} = 8.7 Hz, H₃, H₅), 5.70, 5.53 (s, 2:1, 3 H, CH_{pz}), 3.77, 3.34 (s, 6 H each, CO₂Me), 3.07 (s, 6 H, NMe₂), 2.40, 2.38, 2.07, 1.76 (s, 1:2:1:2, 18 H, Me_{pz}). ¹³C{¹H} NMR (CDCl₃, 25 °C): δ (ppm) 197.2 (C(O)H), 173.6, 166.9 (1:1, CO₂Me), 155.7 (C₄), 157.9, 155.6, 150.4, 149.7 (1:2:2:1, C_{qpz}), 150.4, 143.1 (1:1, CCO₂Me), 142.9 (C₂, C₆), 122.4 (C₁), 111.0 (C₃, C₅), 107.8, 106.4 (2:1, CH_{pz}), 51.5, 50.5 (1:1, CO₂Me), 40.0 (NMe₂), 13.3, 13.2, 12.6, 12.4 (2:1:1:2, Me_{pz}). Anal. Calcd. for C₃₆H₄₅BIrN₇O₉: C, 46.80, H, 4.92, N, 10.62. Found: C, 46.80, H, 4.73, N, 10.87. IR (KBr) ν (cm⁻¹): (CH₃) 2922, 2853, (BH) 2529, (CO₂Me) 1705.

Synthesis of adduct 3d. This compound was prepared following the procedure described above for **3a**, using *p*-nitrobenzaldehyde. Spectroscopic characterization was carried out in the presence of excess free aldehyde in order to prevent the displacement of the aldehyde by adventitious water.



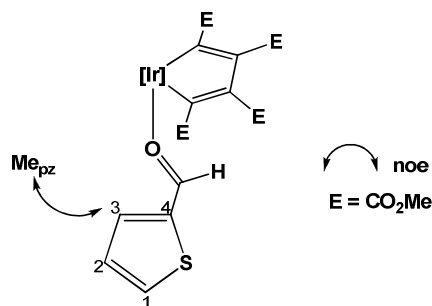
^1H NMR (CDCl_3 , 25 °C): δ (ppm) 10.62 (s, 1 H, C(O)H), 8.26 (d, 2 H, $^3J_{\text{H-H}} = 8.0$ Hz, H₃, H₅), 8.09 (d, 2 H, $^3J_{\text{H-H}} = 8.0$ Hz, H₂, H₆), 5.75, 5.59 (s, 2:1, 3 H, CH_{pz}), 3.78, 3.33 (s, 6 H each, CO₂Me), 2.43, 2.40, 2.09, 1.66 (s, 1:2:1:2, 18 H, Me_{pz}). $^{13}\text{C}\{^1\text{H}\}$ NMR (CDCl_3 , 25 °C): δ (ppm) 205.1 (C(O)H), 172.9, 166.0 (1:1, CO₂Me), 158.5, 150.4 (CCO₂Me), 155.9, 150.2, 143.7, 143.7 (1:2:2:1, C_{qpz}), 151.6 (C₄), 137.5 (C₁), 131.8 (C₂, C₆), 124.7 (C₃, C₅), 108.3, 106.8 (1:2, CH_{pz}), 51.8, 50.8 (1:1, CO₂Me), 13.2, 12.8, 12.4 (3:1:2, Me_{pz}).

Synthesis of adduct 3e. Following the procedure described for **3b**, but using 5-methyl-2-thiophenecarboxaldehyde, the title product was obtained as a red solid, from a cold (-15 °C) Et₂O solution.



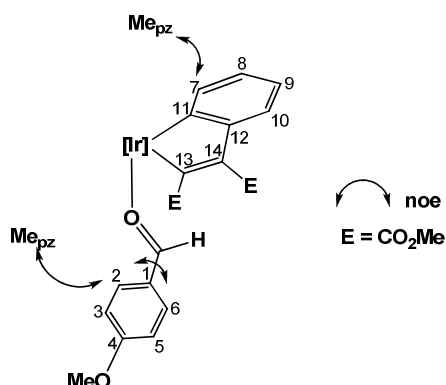
^1H NMR (CDCl_3 , 25 °C): δ (ppm) 9.85 (s, 1 H, C(O)H), 7.88 (d, 1 H, $^3J_{\text{H-H}} = 4.1$ Hz, H₂), 6.88 (d, 1 H, $^3J_{\text{H-H}} = 4.1$ Hz, H₁), 5.70, 5.52 (s, 2:1, 3 H, CH_{pz}), 3.75, 3.33 (s, 6 H each, CO₂Me), 2.45, 2.39, 2.06, 1.78 (s, 1:2:1:2, 18 H, Me_{pz}), 2.26 (s, 3 H, Me_{th}).

Synthesis of adduct 3f. Following the procedure described for **3b**, but adding 2-thiophenecarboxaldehyde, **3f** was obtained as a red solid in *ca.* 85% yield.



^1H NMR (CDCl_3 , 25 °C): δ (ppm) 10.11 (s, 1 H, C(O)H), 8.09 (d, 1 H, $^3J_{\text{H-H}} = 4.1$ Hz, H₃), 7.98 (d, 1 H, $^3J_{\text{H-H}} = 4.3$ Hz, H₁), 7.22 (t, 1 H, $^3J_{\text{H-H}} = 4.3$ Hz, H₂), 5.75, 5.57 (s, 2:1, 3 H, CH_{pz}), 3.79, 3.36 (s, 6 H each, CO₂Me), 2.43, 2.40, 2.10, 1.81 (s, 1:2:1:2, 18 H, Me_{pz}). $^{13}\text{C}\{^1\text{H}\}$ NMR (CDCl_3 , 25 °C): δ (ppm) 194.2 (C(O)H), 173.5, 166.9 (1:1, CO₂Me), 158.4, 150.7 (1:1, CCO₂Me), 156.0, 150.2, 143.6, 143.5 (1:2:2:1, C_{qpz}), 141.4 (C₃), 140.9 (C₁), 140.8 (C₄), 129.7 (C₂), 108.3, 106.8 (1:2, CH_{pz}), 51.9, 50.9 (1:1, CO₂Me), 13.3, 13.2, 12.6, 12.4 (2:1:1:2, Me_{pz}). Anal. Calcd. for C₃₂H₃₈BIrN₆O₉S: C, 43.39, H, 4.32, N, 9.49, S, 3.62. Found: C, 43.46, H, 4.66, N, 9.41, S, 3.8. IR (KBr) ν (cm⁻¹): (Me) 2946, (BH) 2523, (CO₂Me) 1700.

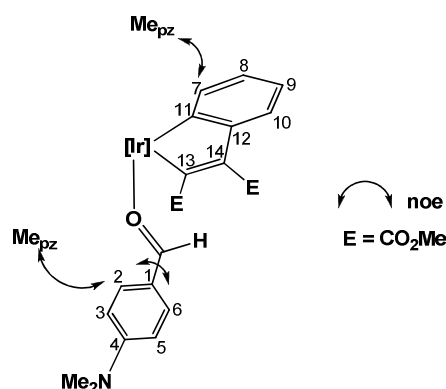
Synthesis of adduct 3(C₆H₄)b. Metallacycle 1(C₆H₄) (0.100 g, 0.12 mmol) was dissolved in CH₂Cl₂ (3 mL) and anisaldehyde (43.8 μL , 0.36 mmol) was added. The mixture was stirred for 2 h at 60 °C, the solvent evaporated under vacuo, and the residue subjected to column chromatography in silica gel, using a mixture Et₂O:hexane (70:30) as the eluent. The title compound was isolated as a red solid in *ca.* 60% yield.



^1H NMR (CDCl_3 , 25 °C): δ (ppm) 9.90 (s, 1 H, C(O)H), 7.67 (d, 2 H, $^3J_{\text{H-H}} = 8.9$ Hz, H₂, H₆), 7.43 (d, 1 H, $^3J_{\text{H-H}} = 7.6$ Hz, H₁₀), 7.08 (d, 1 H, $^3J_{\text{H-H}} = 7.6$ Hz, H₇), 6.89 (t, 1 H, $^3J_{\text{H-H}} = 7.6$ Hz, H₉), 6.81 (d, 1 H,

$^3J_{\text{H-H}} = 8.6$ Hz, H₃, H₅), 6.64 (t, 1 H, $^3J_{\text{H-H}} = 7.2$ Hz, H₈), 5.81, 5.75, 5.45 (s, 1 H each, CH_{pz}), 3.35, 3.83 (s, 3 H each, CO₂Me), 3.82 (s, 3 H, OMe), 2.43, 2.42, 2.40, 1.77, 1.75, 1.37 (s, 3 H each, Me_{pz}). $^{13}\text{C}\{^1\text{H}\}$ NMR (CDCl₃, 25 °C): δ (ppm) 201.0 (C(O)H), 174.6, 167.9 (CO₂Me), 166.3 (C₄), 155.8 (C₁₁), 155.0, 150.7, 150.0, 143.4, 143.4, 143.2 (C_{qpz}), 154.0, 150.7 (C₁₃, C₁₄), 147.4 (C₁₂), 137.6 (C₇), 134.0 (C₂, C₆), 128.0 (C₁), 123.8 (C₁₀), 123.4 (C₈), 122.7 (C₉), 114.9 (C₃, C₅), 108.0, 107.2, 106.4 (CH_{pz}), 55.9 (OMe), 51.6, 50.7 (CO₂Me), 14.2, 13.4, 13.0, 12.6, 12.5 (1:1:1:2:1, Me_{pz}). Anal. Calcd. for C₃₅H₄₀BN₆O₆Ir: C, 49.82, H, 4.78, N, 9.96. Found: C, 49.82, H, 4.71, N, 10.25. IR (KBr) ν (cm⁻¹): (Me) 2919, 2850, (BH) 2522, (CO₂Me) 1711, 1687.

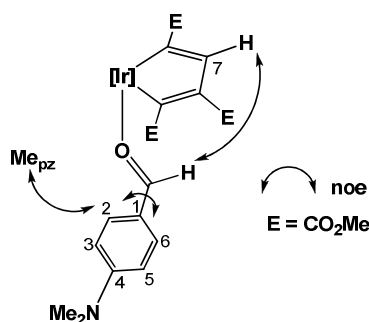
Synthesis of adduct 3(C₆H₄)c. Following the procedure used for compound 3(C₆H₄)b, but using *p*-dimethylaminobenzaldehyde, compound 3(C₆H₄)c was obtained as a red solid in *ca.* 60% yield.



^1H NMR (CDCl₃, 25 °C): δ (ppm) 9.48 (s, 1 H, C(O)H), 7.50 (d, 2 H, $^3J_{\text{H-H}} = 8.7$ Hz, H₂, H₆), 7.44 (d, 1 H, $^3J_{\text{H-H}} = 7.5$ Hz, H₁₀), 7.09 (d, 1 H, $^3J_{\text{H-H}} = 7.5$ Hz, H₇), 6.88 (t, 1 H, $^3J_{\text{H-H}} = 7.5$ Hz, H₉), 6.63 (t, 1 H, $^3J_{\text{H-H}} = 7.5$ Hz, H₈), 6.48 (d, 2 H, $^3J_{\text{H-H}} = 8.7$ Hz, H₃, H₅), 5.80, 5.74, 5.43 (s, 1 H each, CH_{pz}), 3.83, 3.37 (s, 3 H each, CO₂Me), 3.27 (s, 6 H, NMe₂), 2.43, 2.41, 2.39, 1.81, 1.79, 1.36 (s, 3 H each, Me_{pz}). $^{13}\text{C}\{^1\text{H}\}$ NMR (CDCl₃, 25 °C): δ (ppm) 197.2 (C(O)H), 174.7, 167.6 (CO₂Me), 156.0 (C₁₁), 155.2 (C₄), 154.7, 150.1, 150.0, 143.0, 142.9, 142.8 (C_{qpz}), 154.7, 149.8 (C₁₃, C₁₄), 147.3 (C₁₂), 137.1 (C₇), 130.8, 128.7 (C₂, C₆), 123.3 (C₁₀), 123.0 (C₈), 122.7 (C₁), 122.1 (C₉), 110.8 (C₃, C₅), 107.7, 106.2, 106.2 (CH_{pz}), 51.3, 50.4 (CO₂Me), 40.0 (NMe₂), 14.1, 14.0, 13.2, 12.9, 12.4, 12.3 (Me_{pz}). At 25 °C, the rotation around the Ar-C(=O)H bond is on the slow exchange regime on the ^{13}C NMR time scale. Anal.

Calcd. for $C_{36}H_{43}BIrN_7O_5$: C, 50.47, H, 5.06, N, 11.44. Found: C, 50.51, H, 5.29, N, 11.52. IR (KBr) ν (cm^{-1}): (Me) 2973, 2928, (BH) 252, (CO₂Me) 1716, 1685.

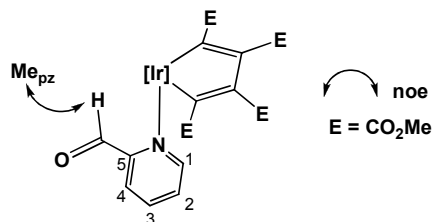
Synthesis of adduct 3(H)c. A sample of compound **3(H)** (0.100 g, 0.134 mmol) was dissolved in CH₂Cl₂ (3 mL) and *p*-dimethylaminobenzaldehyde was added (0.061 g, 0.40 mmol). The mixture was stirred for 2 h at 60 °C, the solvent eliminated under vacuo and the residue extracted with Et₂O. After cooling at -20 °C, red microcrystals of the title compound were isolated in *ca.* 75% yield.



¹H NMR (CDCl₃, 25 °C): δ (ppm) 9.33 (s, 1 H, C(O)H), 8.04 (s, 1 H, H₇), 7.57 (d, 2 H, ³J_{H-H} = 8.7 Hz, H₂, H₆), 6.53 (d, 2 H, ³J_{H-H} = 8.7 Hz, H₃, H₅), 5.71, 5.49 (s, 2:1, 3 H, CH_{pz}), 3.76, 3.42, 3.35 (s, 3 H each, CO₂Me), 3.06 (s, 6 H, NMe₂), 2.39, 1.97, 1.83, 1.64 (s, 3:1:1:1, 18 H, Me_{pz}). ¹³C{¹H} NMR (CDCl₃, 25 °C): δ (ppm) 197.1 (C(O)H), 176.1, 172.4, 164.4 (CO₂Me), 174.1, 145.8, 143.5 (CCO₂Me), 155.4 (C₄), 155.4, 150.8, 149.9, 143.2, 142.9, 142.6 (C_{qpz}), 152.6 (C₇, ¹J_{C-H} = 160 Hz), 122.4 (C₁), 110.9 (v br, C₃, C₅), 107.6, 106.6, 106.0 (CH_{pz}), 51.1, 50.5, 50.5 (CO₂Me), 40.0 (NMe₂), 13.5, 13.3, 12.9, 12.8, 12.4, 12.4 (Me_{pz}). C₂ and C₆ were not located because of their broadness. At 25 °C, the rotation around the Ar–C(=O)H bond is on the intermediate exchange regime on the ¹³C NMR time scale. Anal. Calcd. for $C_{34}H_{43}BIrN_7O_7$: C, 47.22, H, 5.01, N, 11.34. Found: C, 47.26, H, 5.24, N, 11.15. IR (KBr) ν (cm^{-1}): (Me) 2921, (BH) 2528, (CO₂Me) 1697.

Synthesis of adduct 4. Compound **1** (0.100 g, 0.126 mmol) was dissolved in CH₂Cl₂ (3 mL) and 2-pyridinecarboxaldehyde was added (37 μ l, 0.38 mmol). After stirring for 2 h at 60 °C, the solvent was evaporated under vacuo and the residue washed with cold diethyl ether. Crystallization of the resulting

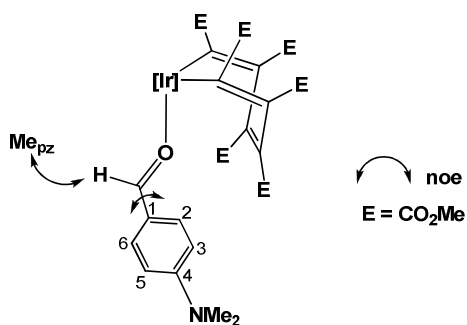
dark yellow solid from a mixture of CH₂Cl₂ and Et₂O, at -20 °C, yielded analytically pure **4** in *ca.* 90% yield.



¹H NMR (CDCl₃, 25 °C): δ (ppm) 9.17 (d, 1 H, ³J_{H-H} = 5.9 Hz, H₁), 7.89 (t, 1 H, ³J_{H-H} = 7.5 Hz, H₃), 7.74 (d, 1 H, ³J_{H-H} = 7.7 Hz, H₄), 7.56 (t, 1 H, ³J_{H-H} = 7.2 Hz, H₂), 6.90 (s, 1 H, C(O)H), 5.82, 5.64 (s, 2:1, 3 H, CH_{pz}), 3.76, 3.34 (s, 6 H each, CO₂Me), 2.51, 2.45, 2.16, 1.19 (s, 2:1:1:2, 18 H, Me_{pz}).

¹³C{¹H} NMR (CDCl₃, 25 °C): δ (ppm) 187.4 (C(O)H), 173.3, 167.2 (1:1, CO₂Me), 156.5 (C₅), 155.5, 151.8 (1:1, CCO₂Me), 156.1, 151.4, 146.4, 143.9 (1:2:2:1, C_{qpz}), 154.7 (C₁), 138.2 (C₃), 128.3 (C₂), 127.5 (C₄), 109.3, 108.2 (2:1, CH_{pz}), 51.9, 50.9 (1:1, CO₂Me), 13.7, 13.4, 13, 12.8 (1:1:2:2, Me_{pz}). Anal. Calcd. for C₃₃H₃₉BIrN₇O₉: C, 45.00, H, 4.46, N, 11.13. Found: C, 44.99, H, 4.15, N, 11.35. IR (KBr) ν (cm⁻¹): (Me) 2943, (BH) 2528, (CO₂Me) 1720, 1696.

Synthesis of adduct 6c. Compound **5** (0.100 g, 0.1 mmol) was dissolved in CH₂Cl₂ (3 mL), *p*-dimethylaminobenzaldehyde was added (0.045 g, 0.3 mmol) and the mixture was stirred at 60 °C for 18 h. After this period of time, the solvent was eliminated under vacuo, and the residue extracted with Et₂O. After cooling at -20 °C, orange crystals of compound **6c** were isolated in *ca.* 85% yield.

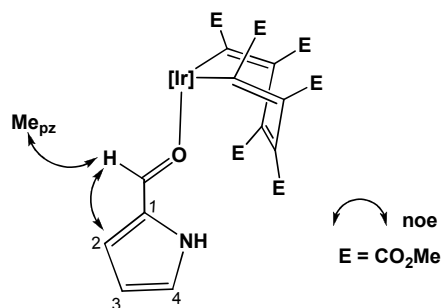


¹H NMR (CDCl₃, 25 °C): δ (ppm) 8.16 (s, 1 H, C(O)H), 8.08, 7.12 (d, 1 H each, ³J_{H-H} = 8.1 Hz, H₂, H₆), 6.73, 6.42 (d, 1 H each, ³J_{H-H} = 7.9 Hz, H₃, H₅), 5.71, 5.65 (s, 2:1, 3 H, CH_{pz}), 3.65, 3.07 (s, 2:1, 18 H, CO₂Me), 3.11 (s, 6 H, NMe₂), 2.39, 2.37, 2.18, 1.84 (s, 2:1:1:2, 18 H, Me_{pz}).

¹³C{¹H} NMR (CDCl₃,

25 °C): δ (ppm) 199.3 (C(O)H), 176.2, 169.3, 167.1 (1:1:1, CO₂Me), 156.0 (C₄), 155.8, 150.9, 143.9, 143.4 (1:2:1:2, C_{qpz}), 152.1, 136.6, 134.4 (1:1:1, CCO₂Me), 138.4, 132.3 (C₂, C₆), 123.2 (C₁), 112.3, 109.8 (C₃, C₅), 107.0, 106.8 (2:1, CH_{pz}), 51.9, 51.7, 50.7 (1:1:1, CO₂Me), 40.3 (NMe₂), 17.5, 13.6, 13.5, 12.7 (1:2:1:2, Me_{pz}). Anal. Calcd. for C₄₂H₅₁BIrN₇O₁₃: C, 47.37, H, 4.83, N, 9.21. Found: C, 47.36, H, 4.70, N, 9.05. IR (KBr) ν (cm⁻¹): (CH₃) 2945, (BH) 2528, (CO₂Me) 1720.

Synthesis of adduct 6g. Following the procedure described for compound **6c** but using pyrrole-2-carboxaldehyde, a crude residue of a dark yellow material was obtained. The title compound was obtained in *ca.* 80% yield after washing this solid with cold (-15 °C) pentane.



¹H NMR (CDCl₃ 25 °C): δ (ppm) 11.84 (s, 1 H, NH), 8.08 (s, 1 H, C(O)H), 7.39 (s, 1 H, H₄), 6.84 (s, 1 H, H₂), 6.27 (s, 1 H, H₃), 5.71, 5.64 (s, 2:1, 3 H, CH_{pz}), 3.64, 3.62, 3.04 (s, 6 H each, CO₂Me), 2.37, 2.15, 1.84 (s, 3:1:2, 18 H, Me_{pz}). ¹³C{¹H} NMR (CDCl₃, 25 °C): δ (ppm) 185.5 (C(O)H), 175.7, 170.9, 166.8 (1:1:1, CO₂Me), 155.6, 150.6, 143.7, 143.4 (1:2:1:2, C_{qpz}), 152.7, 135.8, 134.3 (1:1:1, CCO₂Me), 132.8 (C₄), 131.9 (C₁), 126.4 (C₂), 112.8 (C₃), 106.7, 106.6 (2:1, CH_{pz}), 51.2, 51.6, 50.5 (1:1:1, CO₂Me), 17.3, 13.3, 13.2, 12.5 (1:2:1:2, Me_{pz}). Anal. Calcd. for C₃₈H₄₅BIrN₇O₁₃: C, 45.15, H, 4.49, N, 9.70. Found: C, 45.15, H, 4.50, N, 9.47. IR (KBr) ν (cm⁻¹): (Me) 2984, 2947, (BH) 2530, (CO₂Me) 1722.

Structural Analysis of Complexes 2a, 3b, and 6c·2CH₂Cl₂. X-ray data were collected for all complexes on a Bruker SMART CCD diffractometer equipped with a normal focus, 2.4 kW sealed tube source (Mo radiation, $\lambda = 0.71073$ Å) operating at 50 kV and 40 mA. Data were corrected for absorption by using a multi-scan method applied with the SADABS program.²⁴ The structures of all compounds

were solved by heavy atom methods. Refinement, by full-matrix least squares on F^2 with SHELXL97,²⁵ was similar for all complexes, including isotropic and subsequently anisotropic displacement parameters. The hydrogen atoms were calculated and refined using a restricted riding model. For **6c**·2(CH₂Cl₂) we observed a disordered solvent molecule with occupancies 62:38.

Crystal data for **2a**: C₃₄H₄₀BIrN₆O₉, M_w 879.73, orange, irregular block (0.25 × 0.25 × 0.17), triclinic, space group P-1, *a*: 10.2762(8) Å, *b*: 11.2916(9) Å, *c*: 16.7440(13) Å, α : 83.727(2)°, β : 115.4760(10)°, γ : 115.4760(10)°, *V* = 1826.5(2) Å³, *Z* = 2, *D*_{calc} = 1.600 g cm⁻³, *F*(000) = 880, *T* = 295(2) K, μ = 3.716 mm⁻¹. 22520 measured reflections (2θ : 1.28–26.13°, ω scans 0.3°), 7191 unique (*R*_{int} = 0.0455). Min/max transmission factors: 0.5707/0.4569. Final agreement factors were *R*¹ = 0.0362 (6125 observed reflections, *I* > 2σ(*I*)) and *wR*² = 0.0851. Data/restraints/parameters: 7191/0/470; GoF = 1.113. Largest diff. peak and hole: 1.549 and -0.675 eÅ⁻³.

Crystal data for **3b**: C₃₅H₄₂BIrN₆O₁₀, M_w 909.76, orange, irregular block (0.40 × 0.23 × 0.08), monoclinic, space group P2(1)/c, *a*: 10.0506(12) Å, *b*: 18.310(2) Å, *c*: 22.032(3) Å, β : 100.479(3)°, *V* = 3986.9(9) Å³, *Z* = 4, *D*_{calc} = 1.516 g cm⁻³, *F*(000) = 1824, *T* = 295(2) K, μ = 3.409 mm⁻¹. 26177 measured reflections (2θ : 1.46–26.11°, ω scans 0.3°), 7863 unique (*R*_{int} = 0.0820). Min/max transmission factors: 0.7721/0.3425. Final agreement factors were *R*¹ = 0.0513 (5047 observed reflections, *I* > 2σ(*I*)) and *wR*² = 0.1142. Data/restraints/parameters: 7863/0/489; GoF = 1.045. Largest diff. peak and hole: 1.634 and -1.016 eÅ⁻³.

Crystal data for **6c**·2CH₂Cl₂: C₄₄H₅₅BCl₄IrN₇O₁₃, M_w 1234.76, orange, irregular block (0.61 × 0.54 × 0.47), monoclinic, space group P2(1)/n, *a*: 13.507(3) Å, *b*: 20.843(4) Å, *c*: 19.049(4) Å, β : 103.087(5)°, *V* = 5223.2(17) Å³, *Z* = 4, *D*_{calc} = 1.570 g cm⁻³, *F*(000) = 2488, *T* = 295(2) K, μ = 2.827 mm⁻¹. 32001 measured reflections (2θ : 1.47–25.15°, ω scans 0.3°), 9319 unique (*R*_{int} = 0.0424). Min/max transmission factors: 0.3500/0.2774. Final agreement factors were *R*¹ = 0.0288 (6916 observed reflections, *I* > 2σ(*I*)) and *wR*² = 0.0654. Data/restraints/parameters: 9319/41/673; GoF = 0.953. Largest diff. peak and hole: 0.987 and -0.520 eÅ⁻³.

Structural Analysis of Complexes 2(C₆H₄)b, 4, and 6g. X-ray data were collected for all complexes on a Bruker Smart APEX I or APEX II CCD diffractometers equipped with a normal focus, 2.4 kW sealed tube source (Mo radiation, $\lambda = 0.71073 \text{ \AA}$) operating at 50 kV and 40(6g)/30(2(C₆H₄)b, 4) mA. Data were collected over the complete sphere. Each frame exposure time were 10s or 20s (6g) covering 0.3° in ω . Data were corrected for absorption by using a multiscan method applied with the SADABS program.²⁴ The structures of all compounds were solved by direct methods. Refinement, by full-matrix least squares on F^2 with SHELXL97,²⁵ was similar for all complexes, including isotropic and subsequently anisotropic displacement parameters. The hydrogen atoms were observed in the least Fourier Maps or calculated, and refined freely or using a restricted riding model. For 2(C₆H₄)b 0.5 molecules of diethyl ether by Ir were found in the least cycles of Fourier in two sites in the asymmetric unit, and were refined with restrained geometry and isotropic displacement parameters.

Crystal data for 2(C₆H₄)b: C₃₅H₄₀BIrN₆O₆, O_{0.5}C₂H₅, M_w 880.80, orange, irregular block (0.15 x 0.14 x 0.11), monoclinic, space group P2₁/n, a : 19.2080(9) Å, b : 20.8774(10) Å, c : 22.3156(11) Å, β : 115.4760(10) °, $V = 8078.7(7) \text{ \AA}^3$, $Z = 8$, D_{calc} : 1.448 g cm⁻³, $F(000)$: 3544, $T = 100(2) \text{ K}$, μ 3.356 mm⁻¹). 87963 measured reflections (2θ : 3-58°, ω scans 0.3°), 21028 unique ($R_{\text{int}} = 0.0456$); min./max. transm. Factors 0.740 /0.862. Final agreement factors were $R^1 = 0.0508$ (16588 observed reflections, $I > 2\sigma(I)$) and $wR^2 = 0.1390$; data/restraints/parameters 21028/7/ 947; GoF = 1.036. Largest peak and hole 5.522 and -2.987 e/ Å³.

Crystal data for 4: C₃₃H₃₉BIrN₇O₉, M_w 880.72, yellow, irregular block (0.18 x 0.16 x 0.14), monoclinic, space group P2₁/c, a : 10.4342(7) Å, b : 18.6223(12) Å, c : 18.3236(12) Å, β : 105.6298(8) °, $V = 3428.8(4) \text{ \AA}^3$, $Z = 4$, D_{calc} : 1.706 g cm⁻³, $F(000)$: 1760, $T = 100(2) \text{ K}$, μ 3.959 mm⁻¹). 42204 measured reflections (2θ : 3-58°, ω scans 0.3°), 8407 unique ($R_{\text{int}} = 0.0412$); min./max. transm. Factors 0.742/0.862. Final agreement factors were $R^1 = 0.0260$ (7076 observed reflections, $I > 2\sigma(I)$) and $wR^2 = 0.0625$; data/restraints/parameters 8407/0/476; GoF = 1.032. Largest peak and hole 1.352 and -0.772 e/ Å³.

Crystal data for **6g**: C₃₈H₄₅BIrN₇O₁₃, M_w 1010.82, yellow, plate (0.14 x 0.10 x 0.03), monoclinic, space group C2/c, *a*: 40.649(5) Å, *b*: 11.7275(14) Å, *c*: 17.870(2) Å, β : 105.232(2)°, *V* = 8219.3(17) Å³, *Z* = 8, D_{calc}: 1.634 g cm⁻³, F(000): 4064, T = 100(2) K, μ 3.322 mm⁻¹. 35762 measured reflections (2 θ : 3-58°, ω scans 0.3°), 11447 unique (*R*_{int} = 0.0329); min./max. transm. Factors 0.711/0.862. Final agreement factors were *R*¹ = 0.0277 (9212 observed reflections, *I* > 2 σ (*I*)) and *wR*² = 0.0663; data/restraints/parameters 11447/0/572; GoF = 1.008. Largest peak and hole 1.763 and -0.587 e/ Å³.

Computational details. All calculations were performed with the GAUSSIAN 09 series of programs²⁶ using the B3Lyp functional.^{27,28} An effective core potential²⁹ and its associated double- ζ LANL2DZ³⁰ basis set were used for iridium. C, H, B, N and O atoms were represented by means of the 6-31G(d,p) basis set.³¹⁻³³ The steric effects of the methyl fragments of the Tp^{Me2} ligand were accounted for by means of ONIOM(B3Lyp:UFF) calculations.³⁴⁻³⁶ The structures of the reactants, intermediates, transition states, and products were fully optimized in gas phase without any symmetry restriction. Frequency calculations were performed on all optimized structures at the same level of theory to characterize the stationary points and the transition states, as well as for the calculation of gas-phase enthalpies (*H*), entropies (*S*), and Gibbs energies (*G*) at 298.15 K. The nature of the intermediates connected was determined by perturbing the transition states along the TS coordinate and optimizing to a minimum.

ASSOCIATED CONTENT

Supporting Information. Cif file for compounds **2a**, **2(C₆H₄)b**, **3b**, **4**, **6c·2CH₂Cl₂** and **6g**, and tables of the optimized geometries for the calculated species.

ACKNOWLEDGMENT

Financial support (FEDER and ESF contribution) from the Spanish Ministry of Science (Projects CTQ2010-17476, CTQ2011-23459, and Consolider-Ingenio 2010 CSD2007-00006), the Junta de Andalucía (Grant FQM-119 and Project P09-FQM-4832), the Diputación General de Aragón (E35) and the CONACYT-México (grants 025424 and 84453, and scholarship to A. E. R.) is gratefully acknowledged. J. L.-S. is thankful to the Spanish Ministry of Science and Innovation (MICINN) for a Ramón y Cajal Contract. The use of computational facilities of the Consejo Superior de Investigaciones Científicas (CSIC, Cluster Trueno) and the Supercomputing Centre of Galicia (CESGA) is also acknowledged.

Corresponding author

*E-mail: paneque@iiq.csic.es (M.P.); salazar@uaeh.edu.mx (V.S)

REFERENCES

(1) (a) Tsuji, J.; Ohno, K. *Tetrahedron Lett.* **1965**, 3969-3971. (b) Ohno, K.; Tsuji, J. *J. Am. Chem. Soc.* **1968**, *90*, 99-107. (c) Doughty, D. H.; Pignolet, L. H. *J. Am. Chem. Soc.* **1978**, *100*, 7083-7085. (d) Iwai, T.; Fujihara, T.; Tsuji, Y. *Chem. Commun.* **2008**, 6215-6217. (e) Fristrup, P.; Kreis, M.; Palmelund, A.; Norrby, P.-O.; Madsen, R. *J. Am. Chem. Soc.* **2008**, *130*, 5206-5215.

(2) March, J. *Advanced Organic Chemistry Reactions, Mechanisms and Structure*, 4th ed.; John Wiley and Sons, 1992.

(3) See for example: (a) Shuai, Q.; Yang, L.; Guo, X.; Baslé, O.; Li, Ch.-J. *J. Am. Chem. Soc.* **2010**, *132*, 12212-12213. (b) Wang, J.; Guo, X.; Li, Ch.-J. *J. Organomet. Chem.* **2011**, *696*, 211-215. (c) Guo, X.; Wang, J.; Li, Ch.-J. *J. Am. Chem. Soc.* **2009**, *131*, 15092-15093. (d) Yang, L.; Guo, X.; Li, Ch.-J. *Adv. Synth. Catal.* **2010**, *352*, 2899-2904. (e) Obara, Y.; Anno, Y.; Okamoto, R.; Matsu-ura, T.; Ishii, Y. *Angew. Chem.* **2011**, *123*, 8777-8781. (f) Yang, L.; Zeng, T.; Shuai, Q.; Guo, X.; Li, Ch.-J. *Chem. Commun.* **2011**, *47*, 2161-2163.

- (4) Tejel, C.; Ciriano, M. A.; Passarelli, V. *Chem. Eur. J.* **2011**, *17*, 91-95.
- (5) Geilen, F. M. A.; Stein, T. vom; Engendahl, B.; Winterle, S.; Liauw, M. A.; Klankermayer, J.; Leitner, W. *Angew. Chem. Int. Ed.* **2011**, *50*, 6831-6834.
- (6) (a) Khan, H. A.; Kou, K. G. M.; Dong, V. M. *Chem. Sci.* **2011**, *2*, 407-410. (b) Fessard, T. C.; Andrews, S. P.; Motoyoshi, H.; Carreira, E. M. *Angew. Chem. Int. Ed.* **2007**, *46*, 9331-9334.
- (7) See for example: Rodrigues, C. A. B.; Matos, M. N. de; Guerreiro, B. M. H.; Gonçalves, A. M. L.; Romão, C. C.; Afonso, C. A. M. *Tetrahedron Lett.* **2011**, *52*, 2803-2807, and references therein.
- (8) Garralda, M. A. *Dalton Trans.* **2009**, 3635-3645.
- (9) (a) Alaimo, P. J.; Arndtsen, B. A.; Bergman, R. G. *J. Am. Chem. Soc.* **1997**, *119*, 5269-5270. (b) Alaimo, P. J.; Arndtsen, B. A.; Bergman, R. G. *Organometallics* **2000**, *19*, 2130-2143.
- (10) Gutiérrez-Puebla, E.; Monge, A.; Paneque, M.; Poveda, M. L.; Salazar, V.; Carmona, E. *J. Am. Chem. Soc.* **1999**, *121*, 248-249.
- (11) Alías, F. M.; Daff, P. J.; Paneque, M.; Poveda, M. L.; Carmona, E.; Pérez, P. J.; Salazar, V.; Alvarado, Y.; Atencio, R.; Sánchez-Delgado, R. *Chem. Eur. J.* **2002**, *8*, 5132-5146.
- (12) Roa, A. E.; Salazar, V.; López-Serrano, J.; Oñate, E.; Paneque, M.; Poveda, M. L. *Organometallics* **2012**, *31*, 716-721.
- (13) Paneque, M.; Poveda, M. L.; Rendón, N.; Mereiter, K. *J. Am. Chem. Soc.* **2004**, *126*, 1610-1611.
- (14) (a) Paneque, M.; Posadas, C. M.; Poveda, M. L.; Rendón, N.; Álvarez, E.; Mereiter, K. *Chem. Eur. J.* **2007**, *13*, 5160-5172. (b) Compound **1**·(NC₅H₅) was prepared from **1** and NC₅H₅ following the procedure described in refer. 14a for the NCMe derivative.
- (15) This compound was obtained using a procedure similar to that reported for the CO₂Bu^t derivative (Padilla, R.; Salazar, V.; Paneque, M.; Alvarado-Rodríguez, J. G.; Tamariz, J.; Pacheco-Cuvas, H.;

Vattier, F. *Organometallics* **2010**, *29*, 2835) and was stable enough to be prepared, kept in solid under N₂ atmosphere, and used as a precursor. A full report on this compound will be reported elsewhere.

(16) Álvarez, E.; Paneque, M.; Poveda, M. L.; Rendón, N. *Angew. Chem. Int. Ed.* **2006**, *45*, 474-477.

(17) Paneque, M.; Poveda, M. L.; Rendón, N.; Mereiter, K. *Organometallics*, **2009**, *28*, 172-180.

(18) Huang, Y.-H.; Gladysz, J. A. *J. Chem. Ed.*, **1988**, *65*, 298.

(19) Conejero, S.; López-Serrano, J.; Paneque, M.; Petronilho, A.; Poveda, M. L.; Vattier, F.; Álvarez, E.; Carmona, E. *Chem. Eur. J.* **2012**, in press, DOI: 10.1002/chem.201103507.

(20) Monti, D.; Bassetti, M. *J. Am. Chem. Soc.* **1993**, *115*, 4658-4664.

(21) (a) Álvarez, E.; Conejero, S.; Paneque, M.; Petronilho, A.; Poveda, M. L.; Serrano, O.; Carmona, E. *J. Am. Chem. Soc.* **2006**, *128*, 13060. (b) E. Álvarez, E.; Conejero, S.; Lara, P.; López, J. A.; Paneque, M.; Petronilho, A.; Poveda, M. L.; del Rio, D.; Serrano, O.; Carmona, E. *J. Am. Chem. Soc.* **2007**, *129*, 14130. (c) Conejero, S.; Lara, P.; Paneque, M.; Petronilho, A.; Poveda, M. L.; Serrano, O.; Vattier, F.; Álvarez, E.; Maya, C.; Salazar, V.; Carmona, E. *Angew. Chem. Int. Ed.* **2008**, *47*, 4380. (d) Paneque, M.; Poveda, M. L.; Vattier, F.; Álvarez, E.; Carmona, E. *Chem. Commun.* **2009**, 5561.

(22) Paneque, M.; Posadas, C. M.; Poveda, M. L.; Rendón, N.; Santos, L. L.; Álvarez, E.; Salazar, V.; Mereiter, K.; Oñate, E. *Organometallics* **2007**, *25*, 3403-3415.

(23) Álvarez, E.; Gómez, M.; Paneque, M.; Posadas, C. M.; Poveda, M. L.; Rendón, N.; Santos, L. L.; Rojas-Lima, S.; Salazar, V.; Mereiter, K.; Ruiz, C. *J. Am. Chem. Soc.* **2003**, *125*, 1478-1479.

(24) Blessing, R. H. *Acta Crystallogr.* **1995**, *A51*, 33. SADABS: Area-detector absorption correction; Bruker- AXS, Madison, WI, 1996.

(25) SHELXTL Package v. 6.14; Bruker-AXS, Madison, WI, 2000. Sheldrick, G. M. *Acta Cryst.* **2008**, *A64*, 112-122.

(26) Gaussian 09, Revision B.01, Frisch, M. J.; Trucks, G. W.; Schlegel, H. B.; Scuseria, G. E.; Robb, M. A.; Cheeseman, J. R.; Scalmani, G.; Barone, V.; Mennucci, B.; Petersson, G. A.; Nakatsuji, H.; Caricato, M.; Li, X.; Hratchian, H. P.; Izmaylov, A. F.; Bloino, J.; Zheng, G.; Sonnenberg, J. L.; Hada, M.; Ehara, M.; Toyota, K.; Fukuda, R.; Hasegawa, J.; Ishida, M.; Nakajima, T.; Honda, Y.; Kitao, O.; Nakai, H.; Vreven, T.; Montgomery Jr., J. A.; Peralta, J. E.; Ogliaro, F.; Bearpark, M.; Heyd, J. J.; Brothers, E.; Kudin, K. N.; Staroverov, V. N.; Keith, T.; Kobayashi, R.; Normand, J.; Raghavachari, K.; Rendell, A.; Burant, J. C.; Iyengar, S. S.; Tomasi, J.; Cossi, M.; Rega, N.; Millam, J. M.; Klene, M.; Knox, J. E.; Cross, J. B.; Bakken, V.; Adamo, C.; Jaramillo, J.; Gomperts, R.; Stratmann, R. E.; Yazyev, O.; Austin, A. J.; Cammi, R.; Pomelli, C.; Ochterski, J. W.; Martin, R. L.; Morokuma, K.; Zakrzewski, V. G.; Voth, G. A.; Salvador, P.; Dannenberg, J. J.; Dapprich, S.; Daniels, A. D.; Farkas, O.; Foresman, J. B.; Ortiz, J. V.; Cioslowski, J.; Fox, D. J. *Gaussian, Inc.*, Wallingford CT, 2009.

(27) Becke, A. D. *J. Chem. Phys.* **1993**, *98*, 5648-5652.

(28) Lee, C.; Yang, W.; Parr, R. G. *Phys. Rev. B: Condens. Matter Mater. Phys.* **1988**, *37*, 785.

(29) Hay, P. J.; Wadt, W. R. *J. Chem. Phys.* **1985**, *82*, 299-310.

(30) Höllwart, A.; Böhme, M.; Dapprich, S.; Ehlers, A. W.; Gobbi, A.; Jonas, V.; Köhler, K. F.; Stegmann, R.; Veldkamp, A.; Frenking, G. *Chem. Phys. Lett.* **1993**, *208*, 237-240.

(31) Hehre, W. J.; Ditchfield, R.; Pople, J. A. *J. Phys. Chem.* **1972**, *56*, 2257-2261.

(32) Hariharan, P. C.; Pople, J. A. *Theor. Chim. Acta* **1973**, *28*, 213-222.

(33) Francl, M. M.; Pietro, W. J.; Hehre, W. J.; Binkley, J. S.; Gordon, M. S.; DeFrees, D. J.; Pople, J. A. *J. Chem. Phys.* **1982**, *77*, 3654-3665.

(34) Maseras, F.; Morokuma, K. *J. Comput. Chem.* **1995**, *16*, 1170-1179.

(35) Svensson, M.; Humbel, S.; Froese, R. D. J.; Matsubara, T.; Sieber, S.; Morokuma, K. *J. Phys. Chem.* **1996**, *100*, 19357-19363.

(36) Dapprich, S.; Komáromi, I.; Byun, K. S.; Morokuma, K.; Frisch, M. J. *J. Mol. Struct.: THEOCHEM* **1999**, 461-462, 1.

SYNOPSIS TOC. The fully CO₂Me-substituted iridacyclopentadiene **1** reacts with aromatic aldehydes with formation of *O*-coordinated adducts, which eventually transform into bicyclic Fischer carbenes with the newly created C—H and O—C bonds having an *anti* disposition.

Graphic for the TOC:

